Updating an uncertain and expensive computational model in structural dynamics based on one single target FRF using a probabilistic learning tool

Olivier Ezvan, Christian Soize, Christophe Desceliers, Roger Ghanem

Updating an uncertain and expensive computational model in structural dynamics based on one single target FRF using a probabilistic learning tool

Olivier Ezvan[a], Christian Soize[a,*], Christophe Desceliers[a], Roger Ghanem[b]

[a] *Univ Gustave Eiffel, MSME UMR 8208, 5 bd Descartes, 77454 Marne-La-Vallée, France*
[b] *University of Southern California, 210 KAP Hall, Los Angeles, CA 90089, USA*

Abstract

The paper presents an appropriate and efficient methodology for updating the control parameters of very large uncertain computational models, which are used for analyzing the linear vibrations in the frequency domain of highly complex structures for which there are an enormous number of intertwined local and global elastic structural modes in the broad frequency band of analysis. Moreover, the numerical cost of a single evaluation of the frequency response functions with the computational model is assumed to be very high and only one experimental frequency response function is available as a target. For decreasing the numerical cost of this challenging problem, a parameterized reduced-order model is constructed. Nevertheless, this reduction is not sufficient to be able to solve the non-convex optimization problem related to the updating. Consequently, for avoiding the call to the computational model, the probabilistic learning on manifolds is used for generating a learned set from a training set, which, coupled with conditional statistics, allows the evaluation of the cost function without calling the computational model. A numerical illustration is presented for validating the proposed methodology.

Keywords: updating, computational dynamics, uncertainties, machine learning, probabilistic learning, PLoM

1. Introduction

(i) Objectives of the paper.

The framework of the developments presented in this paper is that of linear vibrations of highly complex structures for which the uncertain high-dimensional model (HDM) can have 10^8, even 10^9 degrees of freedom (dof). The number of frequency points in the frequency band to analyze the structure is of the order of several thousands, even 10^4. The number of elastic structural modes in the frequency band of analysis is of the order of 10^6 with the simultaneous presence of local and global elastic structural modes. This dynamic system depends on a control

*Corresponding author: Christian Soize, christian.soize@univ-eiffel.fr
Email addresses: olivier.ezvan@univ-eiffel.fr (Olivier Ezvan), christian.soize@univ-eiffel.fr (Christian Soize), christophe.desceliers@univ-eiffel.fr (Christophe Desceliers), ghanem@usc.edu (Roger Ghanem)

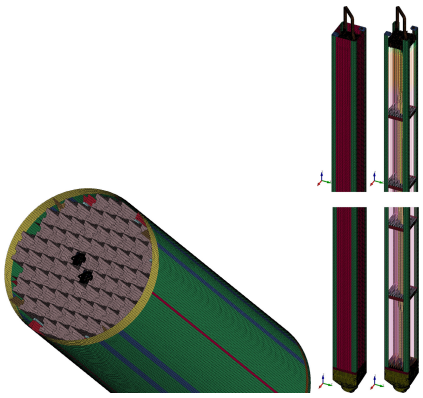

Figure 1: Left: spent nuclear fuel canister loaded with two fuel assemblies – Right: spent nuclear fuel assembly with and without outer shell (pictures from [2])

parameter made up of several hundred parameters, mainly related to local stiffnesses of joints inside the structure. The problem consists in identifying an updated value of the control parameter on the basis of only one available experimental frequency response function (FRF) between one input dof and one output dof located on the boundary of the structure. This updating requires to solve an optimization problem on an admissible set of the control parameter and by using an adapted formulation of the cost function. The admissible set is the support of the prior probability distribution of the uncertain control parameter. This situation, which we have just described, is that of the fully-loaded spent nuclear fuel canisters studied in [1, 2, 3] and depicted in Fig.1. Those are multiscale structures made up of repeated components at various scales, which require fine mesh discretizations and which also exhibit numerous local structural elastic modes that are associated with the isolated vibrations of each of the numerous components. In [3], an HDM was constructed based on nearly half-a-million modes from a finite element model of about 130 million dof. Adapted algorithms were developped allowing a single run of the HDM to be performed in about 40 minutes using a cluster of 50 nodes. In this application, it is of particular interest to be able to perform the updating of physical parameters that describe the structural integrity of the internal components and structural connections, which are critical to nuclear safety.

This challenging problem is particularly difficult because the dynamical system is more than under-observed (in fact only one experimental FRF is available) and one could even think that it is badly posed. However, the FRF is known over a wide frequency band, at a large number of frequency points, which partially removes the under observability. The difficulty of the considered problem also comes from the fact that the numerical cost of one evaluation of a few FRFs with the HDM, for a single fixed value of the control parameter, and for all the frequency points, is huge, even unrealistic.

It is therefore necessary to use a methodology that makes it possible to circumvent these difficulties by considering several ingredients. The first ingredient consists in reducing the numerical cost of a single evaluation of the HDM by constructing a parameterized reduced-order model (ROM) as a function of the control parameter. Such a reduction can be performed either using the proper orthogonal decomposition (POD) of the responses of the dynamic system computed for a given small set of the control parameter values, or using the modal synthesis approach with the parameterized elastic structural modes, formulated with the classical approach or introducing

a multi-frequency model reduction, with or without dynamic substructuring.

The POD approach is very well adapted to nonlinear dynamic systems formulated in the time domain and allows the construction of a basis that is independent of the control parameter, vector basis that is used for projecting the HDM in order to construct a parameterized ROM (see for instance [4, 5, 6, 7, 8, 9, 10, 11, 12, 13]).

Since the problem under consideration is linear and is directly formulated in the frequency domain, we prefer to use the modal synthesis approach, which is based on the elastic structural modes that depend on the control parameter, and which is more accurate in the considered case. For the computational aspects related to the elastic structural modes and modal synthesis, we refer the reader, for instance, to [14, 15, 16] and for the continuum-mechanics aspects to [17]. Due to the presence of a very large number of global and local elastic structural modes in the frequency band of analysis, a multi-frequency model reduction (see [18, 19, 20]) or a multiscale modal analysis [2] could also be used.

For the structures considered, the techniques of dynamic substructuring are often very effective. As explained in the Review Paper [21], the concept of substructures was first introduced by Argyris and Kelsey in 1959 [22] and by Przemieniecki in 1963 [23] who introduced the static boundary functions. This work was extended by Guyan, Irons, and Hurty [24, 25, 26, 27]. Finally, Craig and Bampton in 1968 [28] adapted the Hurty method in order to represent each substructure of the same manner consisting in using the elastic structural modes of the substructure with fixed geometrical interface and the static boundary functions on its geometrical interface. These aspects in the formulation of the continuum mechanics can be found in [17].

For the complex structures under consideration that we have described at the beginning of this section, the simultaneous use of the substructuring technique coupled with a multi-frequency model reduction would be efficient. Nevertheless, in order to simplify the presentation of this paper, we have limited the developments to the framework of the classical modal synthesis without using substructuring technique and multi-frequency model reduction. As the reader will be able to see, the implementation of these two ingredients in the methodology proposed could be performed without significant difficulties.

Even using the parameterized ROM, the numerical cost of a single evaluation of the cost function of the optimization problem, for updating the HDM, is far too high. Indeed, any optimization algorithm for this type of nonconvex problem will have to make a large number of evaluations of the cost function or even of its gradient. This means that it is necessary to build a "surrogate model" that relates the control parameter to the frequency-sampled FRF. Such surrogate models can be chosen in the class of deterministic or statistical representations [29]. There are many methods in the class of deterministic representations based on polynomial and spline regressions or on the use of meshless representations that make it possible to calculate partial derivatives (see for instance [30, 31, 32, 33, 34, 35]). Nevertheless, these methods are not well adapted neither to the high-dimensional problems nor to the statistical framework. For the class of statistical representations, and in particular in the framework of uncertainty quantification [36, 37], there are many possibilities. The use of Gaussian processes to build surrogate models, such as kriging methods, is very popular [38, 39, 40] but these may have limitations induced by high dimensions and by the geometric complexity of the manifold that we seek to represent by a surrogate model. Certainly, another popular method, which is very efficient for many challenging problems, is the use of the polynomial chaos expansion (see for instance [41, 42, 43, 44, 45, 46, 47, 48, 49, 50, 51, 52, 53]). The Bayesian inference could also be considered as a powerful statistical tool for building a surrogate model defined by a statistical inverse problem (see [54, 55, 56, 57, 58, 59, 36, 60] for general aspects and [61, 62, 63, 64, 65, 66, 60]

for more specific aspects related to statistical inverse problems). In the framework of Artificial Intelligence [67], machine learning tools such as the Neural Networks [68] and Deep Learning [69] are very appropriate representations for building surrogate models but generally require big data. For many problems in computational sciences and engineering based on large computational models for simulating physics as a function of a set of control parameters, big data are generally not available due to the high numerical cost for performing a large number of evaluations using the computational model (this is the framework of this paper).

(ii) Strategy used in the paper. In this work, we propose to use the probabilistic learning on manifolds (PLoM) that was proposed in [70, 71, 72] as a complementary approach to existing methods in machine learning for sampling underlying distributions on manifolds [73, 74, 75, 76, 77, 78, 79, 80]. It allows for solving unsupervised and supervised problems under uncertainty for which the training sets are small. As we have already explained, this situation is encountered in many problems of physics and engineering sciences with expensive function evaluations. The PLoM was successfully adapted to tackle these challenges for several related problems including nonconvex optimization under uncertainty [81, 82, 83, 84, 85], updating digital twin [86], calculation of Sobol's indices [87], quantifying uncertainties with small data [88, 89, 90, 91]. More recently, extensions have been proposed for analyzing the case of high stochastic dimension by using the PLoM with partition [72] and also for taking into account constraints in the PLoM algorithm defined by experimental statistical moments [92] or by nonlinear partial differential equations [93], for computational fluid dynamics and nonlinear solid dynamics.

In this paper, we present a methodology for updating the uncertain computational model. As it is well known, the updating problem requires to solve an optimization problem for which several formulations are possible in the statistical context for constructing the "cost function": the least-square method, the maximum likelihood, or the Bayesian approach. The last two cannot easily be used because only one target is available. We address this challenge by using the algorithm that we have presented in [81] and validated in [82, 83, 84], but, on the one hand by replacing the PLoM algorithm [70] by the novel algorithm of PLoM [92, 72] in order to apply the constraints related to the normalization and on the other hand by constructing a cost function on the basis of conditional statistics estimated with the learned set generated with PLoM. This approach allows for maintaining the number of function evaluations at the level essentially equal to that of the construction of the training set.

Finally, the presented numerical application is an illustration, which is representative of all the reported difficulties of the problem posed, but which does not have the complexity of the structures mentioned at the beginning of this paragraph. This choice was made so that the reader can reproduce all the results presented from a simply and completely described dynamic system.

(iii) Novelty of the paper. This paper presents an appropriate and efficient methodology for updating high-dimensional uncertain computational models in the domain of linear vibrations, with a formulation in the frequency domain, for a broad frequency band, for which each evaluation is expensive, and for which only one experimental frequency response function is available as a target. We formulate a nonconvex optimization problem, which is solved using a probabilistic learning tool and conditional statistics, which have been specifically developed for the case of a training set constituted of a small number of points. In this framework, the methodology proposed is novel. It should be noted that we are searching for improving a computational model in the framework of an ill-posed problem, related to the nonconvexity of the optimization problem formulated for the updating, to the under observability, and to the knowledge of only one ex-

perimental FRF. Nevertheless, despite this serious difficulty, we propose an approach that allows for updating the model. As explained in the description of the strategy, the updating is first performed by using the training set. Then, alternatively, the PLoM method is used as a resampling tool for trying to improve the updating with respect to the one given by the training set. Through the presented applications, it will be seen that this additional resampling may or may not improve the updating. The main explanation to this phenomena is not due to the capability of PLoM, but is due to the lack of monotonicity of the optimum solution as a function of the size of the training set. This point will be further discussed in the application.

(iv) Organization of the paper. In Section 2, we list all the hypotheses used for the proposed methodology in order to carry out the updating of the computational model. Section 3 is devoted to the definition of the parameterized computational model for the linear vibrations formulated in the frequency domain. Section 4 deals with the construction of the parameterized ROM that is obtained by projection on the parameterized elastic structural modes. The convergence of the modal synthesis is controlled for each value of the control parameter yielding parameterized ROM whose dimension depends on the control parameter. Section 5 begins with the construction of the probabilistic model of the control parameter. Then the training set is built using the stochastic ROM deduced from the parameterized ROM and the probabilistic model of the control parameter. This training set will allow the learned set to be generated, which will be used to solve the optimization problem. Section 6 deals with the formulation of the updating of the stochastic parameterized ROM. The cost function is constructed with a least-square formulation and the use of the statistical conditioning of the random parameterized frequency response function, given a value of the control parameter. For each value of the control parameter, which is proposed by the optimization algorithm, this statistical conditioning is performed with the learned set generated by PLoM and an algebraic formulation derived from the nonparametric statistics. The numerical application is presented in Section 7. All the numerical values of the parameters and data that are necessary for reproducing the results are given. The results obtained are presented, which are accompanied by a discussion. The PLoM algorithm is summarized in Appendix A.

Notations

Lower-case letters such as q or η are deterministic real variables.
Boldface lower-case letters such as $\mathbf{q}$ or $\boldsymbol{\eta}$ are deterministic vectors.
Upper-case letters such as X or H are real-valued random variables.
Boldface upper-case letters such as $\mathbf{X}$ or $\mathbf{H}$ are vector-valued random variables.
Lower-case letters between brackets such as $[x]$ or $[\eta]$ are deterministic matrices.
Boldface upper-case letters between brackets such as $[\mathbf{X}]$ or $[\mathbf{H}]$ are matrix-valued random variables.

$\delta_{\alpha\beta}$: Kronecker's symbol.
ι: imaginary unit in set $\mathbb{C}$.
n_u: number of dof in the computational model.
n_ω: number of frequency sampling points.
n_w: number of control parameters.
$\mathbb{C}^n$: Hermitian vector space on $\mathbb{C}$ of dimension n.
$[I_n]$: identity matrix in $\mathbb{M}_n$.
$\mathbb{M}_{n,N}$: set of $(n \times N)$ real matrices.
$\mathbb{M}_n$: set of square $(n \times n)$ real matrices.

$\mathbb{M}_n^{+0}$: set of positive symmetric $(n \times n)$ real matrices.
$\mathbb{M}_n^{+}$: set of positive-definite symmetric $(n \times n)$ matrices.
$\mathbb{R}^n$: Euclidean vector space on $\mathbb{R}$ of dimension n.
$[x]_{kj}$: entry of matrix $[x]$.
$[x]^T$: transpose of matrix $[x]$.
$<\mathbf{x}\,,\mathbf{y}>$: Euclidean or Hermitian inner product.
$\|\mathbf{x}\|$: Euclidean or Hermitian norm $<\mathbf{x}\,,\mathbf{x}>^{1/2}$.

2. Hypotheses used for developing the methodology

(H1) We consider the linear structural vibrations of a complex heterogeneous linear mechanical system with respect to the geometry, the boundary conditions, and the materials. We are interested in characterizing the vibrations in the frequency domain Ω that is a bounded interval of $\mathbb{R}$.

(H2) The structure is a multi-scale system inducing the presence of a huge number of local and global elastic structural modes in the frequency band Ω.

(H3) The frequency sampling set $\Omega_s = \{\omega_1, \ldots, \omega_{n_\omega}\} \subset \Omega$ is made up of a large number n_ω of frequency sampling points.

(H4) Due to (H2), the HDM requires the use of a very large number n_u of degrees of freedom.

(H5) The HDM depends on a control parameter $\mathbf{w} = (w_1, \ldots, w_{n_w})$ belonging to an admissible set $C_{\mathbf{w}} \subset \mathbb{R}^{n_w}$ in which n_w is relatively small and for which a nominal value $\underline{\mathbf{w}}$ is given in $C_{\mathbf{w}}$. The control parameter is uncertain and its nominal value must be updated by using experimental information.

(H6) For a fixed value of $\mathbf{w}$ in $C_{\mathbf{w}}$, we consider n_o frequency response functions $\{\omega \mapsto \mathrm{FRF}_k(\omega;\mathbf{w}), k = 1, \ldots, n_o\}$ from Ω into $\mathbb{C}$ in which n_o is relatively small (a few units). The quantity of interest is the real matrix $[q(\mathbf{w})] \in \mathbb{M}_{n_\omega, n_o}$ depending on the control parameter $\mathbf{w}$ and on the frequency sampling such that $[q(\mathbf{w})]_{mk} = 20\,\log_{10}(|\mathrm{FRF}_k(\omega_m;\mathbf{w})|)$ with $m \in \{1, \ldots, n_\omega\}$ and $k \in \{1, \ldots n_o\}$. The numerical cost of one evaluation performed with the HDM is assumed to be high.

(H7) It is assumed that only one experimental FRF (the target) is available and is sampled using the frequency points of Ω_s. This single experimental FRF is associated with the last observation of the HDM whose index is n_o. It means that the number n_o of observations is possibly greater than the number of targets (that is only of one). This sampled experimental FRF is then denoted by $\{\mathrm{FRF}^{\mathrm{targ}}(\omega_m), m = 1, \ldots, n_\omega\}$. The experimental quantity of interest (the target) is then defined as the real vector $\mathbf{q}^{\mathrm{targ}} = (q_1^{\mathrm{targ}}, \ldots, q_{n_\omega}^{\mathrm{targ}}) \in \mathbb{R}^{n_\omega}$ such that $q_m^{\mathrm{targ}} = 20\,\log_{10}(|\mathrm{FRF}^{\mathrm{targ}}(\omega_m)|)$ for $m \in \{1, \ldots, n_\omega\}$.

3. Computational model and frequency response functions

From Hypotheses (H1), (H3), and (H4), the finite element discretization with n_u degrees of freedom of the boundary value problem yields the HDM that is written, in the frequency domain and for $\omega \in \Omega$, as

$$(-\omega^2\,[M(\mathbf{w})] + \imath\,\omega\,[D(\mathbf{w})] + [K(\mathbf{w})])\,\mathbf{u}(\omega;\mathbf{w}) = [B]\,\mathbf{f}(\omega)\,, \tag{1}$$

$$\mathbf{o}(\omega;\mathbf{w}) = [A]\,\mathbf{u}(\omega;\mathbf{w})\,, \tag{2}$$

in which $\mathbf{w} \in C_{\mathbf{w}}$ is the control parameter, $\mathbf{u}(\omega;\mathbf{w}) \in \mathbb{C}^{n_u}$ is the complex vector of the response for all the degrees of freedom, $[M(\mathbf{w})]$, $[D(\mathbf{w})]$, and $[K(\mathbf{w})]$ are the mass, damping, and stiffness matrices that are assumed to be in $\mathbb{M}^+_{n_u}$ (set of all the positive-definite symmetric $(n_u \times n_u)$ real matrices), where $[B]$ is the controllability real matrix in $\mathbb{M}_{n_u,n_f}$ in which n_f is the number of excited dofs, $[A]$ is the observability real matrix in $\mathbb{M}_{n_o,n_u}$, where $\mathbf{f}(\omega)$ is the complex vector of applied loads in $\mathbb{C}^{n_f}$, and where $\mathbf{o}(\omega;\mathbf{w})$ is the complex vector of the observations in $\mathbb{C}^{n_o}$.

Taking into account Hypothesis (H7), let us define n_o frequency response functions $\{\omega \mapsto \text{FRF}_k(\omega;\mathbf{w}) : \Omega \to \mathbb{C}, k = 1,\ldots,n_o\}$, which all have the same input dof, i_{input}, and for which the n_o output dofs are $\{o_k(\omega;\mathbf{w}), k = 1,\ldots,n_o\}$. We then have $n_f = 1$, $\mathbf{f}(\omega) = f(\omega) = 1$ for all ω, and $[B]_{i,1} = \delta_{i,i_{\text{input}}}$ for all $i \in \{1,\ldots,n_u\}$. Therefore, we have, $\text{FRF}_k(\omega;\mathbf{w}) = o_k(\omega;\mathbf{w})$. For $\omega \in \Omega_s$, the quantity of interest is the real matrix $[q(\mathbf{w})] \in \mathbb{M}_{n_\omega,n_o}$ such that $[q(\mathbf{w})]_{mk} = 20\,\log_{10}(|\text{FRF}_k(\omega_m;\mathbf{w})|)$.

4. Parameterized reduced-order model

Due to Hypotheses (H3) (n_ω large) and (H4) (n_u very large), and as we have explained in Section 1, we have to construct a reduced-order model (ROM). However, since the HDM depends on control parameter $\mathbf{w}$, a parameterized ROM has to be built. For that we use the classical approach of modal synthesis consisting in projecting Eqs. (1) and (2) on a finite family of the elastic structural modes of the associated homogeneous conservative system. As we have previously explained, a multi-frequency model reduction with or without substructuring techniques can be used for complex structural dynamics problems, but in this paper, for simplifying the presentation, we limit the development to the classical modal synthesis. For all $\mathbf{w}$ fixed in $C_{\mathbf{w}}$, we introduce the generalized eigenvalue problem associated with Eq. (1),

$$[K(\mathbf{w})]\,[\Phi(\mathbf{w})] = [M(\mathbf{w})]\,[\Phi(\mathbf{w})]\,[\Lambda(\mathbf{w})]\,, \tag{3}$$

in which $[\Lambda(\mathbf{w})]$ is the diagonal matrix of the smallest eigenvalues $0 < \lambda_1(\mathbf{w}) \le \ldots \le \lambda_{N(\mathbf{w})}(\mathbf{w})$ in which $N(\mathbf{w}) \ll n_u$ is defined below by using a convergence criterion. The columns of the matrix $[\Phi(\mathbf{w})]$ in $\mathbb{M}_{n_u,N(\mathbf{w})}$ are the eigenvectors (the elastic structural modes) associated with the eigenvalues that are the square of the eigenfrequencies. This matrix satisfies the usual orthogonality properties $[\Phi(\mathbf{w})]^T\,[M(\mathbf{w})]\,[\Phi(\mathbf{w})] = [I_{N(\mathbf{w})}]$ and $[\Phi(\mathbf{w})]^T\,[K(\mathbf{w})]\,[\Phi(\mathbf{w})] = [\Lambda(\mathbf{w})]$. Introducing the complex vector $\mathbf{v}(\omega;\mathbf{w})$ in $\mathbb{C}^{N(\mathbf{w})}$ of the generalized coordinates such that $\mathbf{u}(\omega;\mathbf{w}) = [\Phi(\mathbf{w})]\,\mathbf{v}(\omega;\mathbf{w})$, the parameterized ROM can then be written as

$$\mathbf{o}(\omega;\mathbf{w},N(\mathbf{w})) = [\mathcal{A}(\mathbf{w})]\,\mathbf{v}(\omega;\mathbf{w},N(\mathbf{w}))\,, \tag{4}$$

$$(-\omega^2\,[I_{N(\mathbf{w})}] + \imath\,\omega\,[\mathcal{D}(\mathbf{w})] + [\Lambda(\mathbf{w})])\,\mathbf{v}(\omega;\mathbf{w},N(\mathbf{w})) = [\mathcal{B}(\mathbf{w})]\,\mathbf{f}(\omega)\,, \tag{5}$$

in which $[\mathcal{A}(\mathbf{w})] = [A][\Phi(\mathbf{w})] \in \mathbb{M}_{n_o,N(\mathbf{w})}$ is the reduced observability matrix, where $[\mathcal{B}(\mathbf{w})] = [\Phi(\mathbf{w})]^T\,[B] \in \mathbb{M}_{N(\mathbf{w}),n_u}$ is the reduced controllability matrix, and where $[\mathcal{D}(\mathbf{w})] = [\Phi(\mathbf{w})]^T\,[D(\mathbf{w})]\,[\Phi(\mathbf{w})] \in \mathbb{M}^+_{N(\mathbf{w})}$ is the positive-definite reduced damping matrix. For estimating $N(\mathbf{w})$, the usual L^2 criterion cannot be used because it requires the computation of $\mathbf{o}(\omega_m;\mathbf{w})$ for all $\omega \in \Omega_s$ by using Eqs. (1) and (2) of the HDM, which is way too expensive. Two methods can be used to analyze the convergence of the ROM with respect to $N(\mathbf{w})$. The first one consists in analyzing the convergence of the sequence $\{\mathbf{o}(\omega;\mathbf{w},N(\mathbf{w}))\}_{N(\mathbf{w})}$ with respect to $N(\mathbf{w})$ by using the following criterion (of the Cauchy type): for ε given independent of $\mathbf{w}$, find $N^{\text{opt}}(\mathbf{w})$ such that for all

$N(\mathbf{w}) \geq N^{\text{opt}}(\mathbf{w})$ and $N'(\mathbf{w}) \geq N^{\text{opt}}(\mathbf{w})$, we have

$$\frac{2\sum_m \|\mathbf{o}(\omega_m;\mathbf{w},N(\mathbf{w})) - \mathbf{o}(\omega_m;\mathbf{w},N'(\mathbf{w}))\|^2}{\sum_m \|\mathbf{o}(\omega_m;\mathbf{w},N(\mathbf{w})) + \mathbf{o}(\omega_m;\mathbf{w},N'(\mathbf{w}))\|^2} \leq \varepsilon\,.$$

The second one is as follows. At the desired cutoff frequency of the modal basis, the LDL factorization of the dynamic stiffness matrix (without damping) is computed. The number of negative terms in the diagonal matrix of this factorization is equal to the number of eigenvalues below the cutoff frequency. This way, for all $\mathbf{w}$, the $N(\mathbf{w})$ structural elastic modes cover the same frequency band. It should thus be noted that the dimension $N^{\text{opt}}(\mathbf{w})$ of the ROM depends on $\mathbf{w}$. In the application presented in Section 7, it is the latter method that will be used.

5. Probabilistic model of the control parameter and generation of the training set using the stochastic parameterized reduced-order model

The control parameter $\mathbf{w} = (w_1, \ldots, w_{n_w})$ with values in $C_{\mathbf{w}} \subset \mathbb{R}^{n_w}$ is modeled by a $\mathbb{R}^{n_w}$-valued random variable $\mathbf{W} = (W_1, \ldots, W_{n_w})$ defined on a probability space $(\Theta, \mathcal{T}, \mathcal{P})$, the probability distribution $P_{\mathbf{W}}(d\mathbf{w})$ of which is given and has a support that is $C_{\mathbf{w}}$. The mean value $\underline{\mathbf{w}} = E\{\mathbf{W}\} = \int_{\mathbb{R}^{n_w}} \mathbf{w}\, P_{\mathbf{W}}(d\mathbf{w})$ of $\mathbf{W}$ is thus known and considered as the nominal value of the control parameter. The random generator of $P_{\mathbf{W}}(d\mathbf{w})$ allows for generating N_d independent realizations $\{\mathbf{w}_d^1, \ldots, \mathbf{w}_d^{N_d}\}$ of $\mathbf{W}$. For each $\mathbf{w}_d^j \in C_{\mathbf{w}}$ with j fixed in $\{1, \ldots, N_d\}$, the parameterized ROM of dimension $N^{\text{opt}}(\mathbf{w}_d^j)$, defined in Section 4, is used for computing the observations and then deducing, using the end of Section 3, the quantity of interest $[q_d^j] \in \mathbb{M}_{n_\omega, n_o}$ such that, for $m = 1, \ldots, n_\omega$ and $k = 1, \ldots, n_o$, we have $[q_d^j]_{mk} = [q(\mathbf{w}_d^j)]_{mk} = 20\,\log_{10}(|\text{FRF}_k(\omega_m; \mathbf{w}_d^j)|)$. The training set is then defined by the N_d independent realizations $\{([q_d^j], \mathbf{w}_d^j),\, j = 1, \ldots, N_d\}$ of random variable $([\mathbf{Q}], \mathbf{W})$ with values in $\mathbb{M}_{n_\omega, n_o} \times \mathbb{R}^{n_w}$. For generating the learned set using the PLoM whose algorithm is summarized in Appendix A, matrix $[q_d^j]$ is reshaped in a vector $\mathbf{q}_d^j \in \mathbb{R}^{n_q}$ with $n_q = n_\omega \times n_o$.

6. Optimization problem for model updating

6.1. Defining the cost function and formulation of the optimization problem for model updating

From Hypotheses (H6) and (H7), the quantity of interest, associated with the one experimental FRF sampled in the n_ω frequency points of Ω_s, is the real vector $\mathbf{q}^{\text{targ}} = (q_1^{\text{targ}}, \ldots, q_{n_\omega}^{\text{targ}})$ belonging to $\mathbb{R}^{n_\omega}$. When computed with the stochastic computational model, the corresponding quantity (see Hypothesis (H7)) is the $\mathbb{R}^{n_\omega}$-valued random variable $([\mathbf{Q}]_{1n_o}, \ldots, [\mathbf{Q}]_{n_\omega n_o})$ such that $[\mathbf{Q}]_{mn_o} = [q(\mathbf{W})]_{mn_o}$ with $m \in \{1, \ldots, n_\omega\}$, which depends on the $\mathbb{R}^{n_w}$-valued random control parameter $\mathbf{W}$.

We propose the following formulation for the model updating. The updated value $\mathbf{w}^{\text{opt}} \in \mathbb{R}^{n_w}$ of the nominal value $\underline{\mathbf{w}} \in \mathbb{R}^{n_w}$ of the control parameter is constructed as the solution of the optimization problem,

$$\mathbf{w}^{\text{opt}} = \arg \min_{\mathbf{w}^0 \in C_{\mathbf{w}}} J(\mathbf{w}^0)\,, \tag{6}$$

in which $C_{\mathbf{w}} \subset \mathbb{R}^{n_w}$ is the admissible set of the control parameter and where J is the cost function.

A first formulation of the cost function could be defined for all $\mathbf{w}^0 \in C_{\mathbf{w}}$ by

$$J(\mathbf{w}^0) = \frac{1}{n_\omega} \sum_{m=1}^{n_\omega} (q_m^{\text{targ}} - E\{[\mathbf{Q}]_{mn_o} \,|\, \mathbf{W} = \mathbf{w}^0\})^2 \,. \tag{7}$$

In Eq. (7), $E\{[\mathbf{Q}]_{mn_o} \,|\, \mathbf{W} = \mathbf{w}^0\}$ is the conditional mathematical expectation of the real-valued random variable $[\mathbf{Q}]_{mn_o}$ given $\mathbf{W} = \mathbf{w}^0$ for $\mathbf{w}^0$ in $C_{\mathbf{w}}$. Since there are no uncontrolled random variables in the considered system, if $\mathbf{W}$ is fixed to a given value $\mathbf{w}^0$, then $[\mathbf{Q}]_{mn_o}$ is deterministic and consequently, the conditional probability measure of $[\mathbf{Q}]_{mn_o}$ given $\mathbf{W} = \mathbf{w}^0$ is a Dirac measure. Nevertheless, since the training set has a finite number N_d of points, the estimation of the joint probability measure of $([\mathbf{Q}]_{mn_o}, \mathbf{W})$ is performed using the Gaussian kernel density estimation method of the nonparametric statistics. Consequently, such a data smoothing allows for introducing a regularization of the joint probability measure whose support is the manifold defined by the graph $\{([\mathbf{q}]_{mn_o}(\mathbf{w}), \mathbf{w}), \mathbf{w} \in C_w\}$. Therefore, the joint probability measure of random variable $([\mathbf{Q}]_{mn_o}, \mathbf{W})$ admits a density with respect to the Lebesgue measure on $\mathbb{R} \times \mathbb{R}^{n_{\mathbf{w}}}$. In the framework of such a smoothing, it can then be assumed that the conditional probability measure of $[\mathbf{Q}]_{mn_o}$ given $\mathbf{W} = \mathbf{w}^0$ can be written as

$$P_{[\mathbf{Q}]_{mn_o}|\mathbf{W}}(dq|\mathbf{w}^0) = p_{[\mathbf{Q}]_{mn_o}|\mathbf{W}}(q|\mathbf{w}^0)\, dq$$

in which $q \mapsto p_{[\mathbf{Q}]_{mn_o}|\mathbf{W}}(q|\mathbf{w}^0)$ is the conditional probability density function of $[\mathbf{Q}]_{mn_o}$ with respect to the Lebesgue measure dq on $\mathbb{R}$, given $\mathbf{W} = \mathbf{w}^0$ (it will be the case, see Section 6.2). Consequently,

$$E\{[\mathbf{Q}]_{mn_o}|\mathbf{W} = \mathbf{w}^0\} = \int_{\mathbb{R}} q\, p_{[\mathbf{Q}]_{mn_o}|\mathbf{W}}(q|\mathbf{w}^0)\, dq. \tag{8}$$

Note that the conditional random variable $[\mathbf{Q}]_{mn_o}|\mathbf{W} = \mathbf{w}^0$ is a $\mathbb{R}$-valued random variable. In general, the maximum of the conditional pdf, $q \mapsto p_{[\mathbf{Q}]_{mn_o}|\mathbf{W}}(q|\mathbf{w}^0)$, is not reached at the mean value $E\{[\mathbf{Q}]_{mn_o} \,|\, \mathbf{W} = \mathbf{w}^0\}$. Hence, there is an interest in considering a second formulation of the cost function that is defined as follows. For $\mathbf{w}^0$ fixed in $C_{\mathbf{w}}$ and for m fixed in $\{1, \ldots, n_\omega\}$, let $q_m^{\text{ML}}(\mathbf{w}^0)$ be defined by

$$q_m^{\text{ML}}(\mathbf{w}^0) = \arg\max_q p_{[\mathbf{Q}]_{mn_o}|\mathbf{W}}(q|\mathbf{w}^0) \,. \tag{9}$$

Therefore, Eq. (7) is replaced by the following one,

$$J(\mathbf{w}^0) = \frac{1}{n_\omega} \sum_{m=1}^{n_\omega} (q_m^{\text{targ}} - q_m^{\text{ML}}(\mathbf{w}^0)\})^2 \,. \tag{10}$$

6.2. Estimating the conditional statistics using PLoM

As previously explained, the PLoM method is used for generating the learned set made up of $N_{\text{ar}} \gg N_d$ realizations $\{([q_{\text{ar}}^\ell], \mathbf{w}_{\text{ar}}^\ell), \ell = 1, \ldots, N_{\text{ar}}\}$ of random variable $([\mathbf{Q}], \mathbf{W})$ with values in $\mathbb{M}_{n_\omega, n_o} \times \mathbb{R}^{n_w}$, without calling the computational model. The PLoM algorithm [70, 71, 92, 72] is summarized in Appendix A, in which the random matrix $[\mathbf{Q}]$ with values in $\mathbb{M}_{n_\omega, n_o}$ is reshaped in the random vector $\mathbf{Q}$ with values in $\mathbb{R}^{n_q}$ with $n_q = n_\omega \times n_o$.

For m fixed in $\{1, \ldots, n_\omega\}$ and for $\mathbf{w}^0$ fixed in $C_{\mathbf{w}}$, the conditional mathematical expectation

$$E\{[\mathbf{Q}]_{mn_o} \,|\, \mathbf{W} = \mathbf{w}^0\}$$

is estimated using the learned set $\{([q^\ell_{\rm ar}]_{mn_o}, \mathbf{w}^\ell_{\rm ar}), \ell = 1, \ldots, N_{\rm ar}\}$. In order to simplify the notation, in this subsection, the subscripts m and n_o will be removed and consequently, $Q_{mn_o} = [\mathbf{Q}]_{mn_o}$, $q_{mn_o} = [q]_{mn_o}$, $\underline{q}_{mn_o} = [\underline{q}]_{mn_o}$, $[q^\ell_{\rm ar}]_{mn_o}$, and so on, will simply be noted as Q, q, $\underline{q}$, $q^\ell_{\rm ar}$, and so on. Let $\underline{q}$ and σ_Q be the empirical mean value and standard deviation of random variable Q estimated with $\{q^\ell_{\rm ar}, \ell = 1, \ldots, N_{\rm ar}\}$. Similarly, for $i \in \{1, \ldots, n_w\}$ let $\underline{w}_i$ and σ_i be the empirical mean value and standard deviation of the real-valued random variable W_i estimated with $\{w^\ell_{{\rm ar},i}, \ell = 1, \ldots, N_{\rm ar}\}$. We introduce the normalized random variables $\widetilde{Q}$ and $\widetilde{\mathbf{W}} = (\widetilde{W}_1, \ldots, \widetilde{W}_{n_w})$ such that, for $i = 1, \ldots, n_w$,

$$Q = \underline{q} + \sigma_Q \, \widetilde{Q} \quad , \quad W_i = \underline{w}_i + \sigma_i \, \widetilde{W}_i \, .$$

We define $\widetilde{\mathbf{w}}^0 = (\widetilde{w}^0_1, \ldots, \widetilde{w}^0_{n_w})$ such that

$$w^0_i = \underline{w}_i + \sigma_i \, \widetilde{w}^0_i \quad , \quad i = 1, \ldots, n_w \, .$$

Consequently, Eqs. (8) and (9) can be calculated by using the following equations,

$$E\{Q \,|\, \mathbf{W} = \mathbf{w}^0\} = \underline{q} + \sigma_Q \, E\{\widetilde{Q} \,|\, \widetilde{\mathbf{W}} = \widetilde{\mathbf{w}}^0\} \, , \tag{11}$$

in which

$$E\{\widetilde{Q} \,|\, \widetilde{\mathbf{W}} = \widetilde{\mathbf{w}}^0\} = \frac{1}{p_{\widetilde{\mathbf{W}}}(\widetilde{\mathbf{w}}^0)} \int_{\mathbb{R}} \widetilde{q} \, p_{\widetilde{Q},\widetilde{\mathbf{W}}}(\widetilde{q}, \widetilde{\mathbf{w}}^0) \, d\widetilde{q} \, , \tag{12}$$

and

$$q^{\rm ML}(\mathbf{w}_0) = \arg\max_{\widetilde{q}} \, p_{\widetilde{Q}|\widetilde{\mathbf{W}}}(\widetilde{q}|\widetilde{\mathbf{w}}^0) \, . \tag{13}$$

In Eq. (12), $p_{\widetilde{\mathbf{W}}}(\widetilde{\mathbf{w}}^0) = \int_{\mathbb{R}} p_{\widetilde{Q},\widetilde{\mathbf{W}}}(\widetilde{q}, \widetilde{\mathbf{w}}^0) \, d\widetilde{q}$ and where $(\widetilde{q}, \widetilde{\mathbf{w}}) \mapsto p_{\widetilde{Q},\widetilde{\mathbf{W}}}(\widetilde{q}, \widetilde{\mathbf{w}})$ is the pdf on $\mathbb{R} \times \mathbb{R}^{n_w}$ of random variable $(\widetilde{Q}, \widetilde{\mathbf{W}})$ with respect to $d\widetilde{q} \, d\widetilde{\mathbf{w}}$. The classical Gaussian KDE method [94, 95, 96, 97] is used for estimating $p_{\widetilde{Q},\widetilde{\mathbf{W}}}(\widetilde{q}, \widetilde{\mathbf{w}})$ on $\mathbb{R} \times \mathbb{R}^{n_w}$ as

$$p_{\widetilde{Q},\widetilde{\mathbf{W}}}(\widetilde{q}, \widetilde{\mathbf{w}}) = \frac{1}{N_{\rm ar}} \sum_{\ell=1}^{N_{\rm ar}} \frac{1}{s_{\rm SB} \sqrt{2\pi}} \exp\{-\frac{1}{2 s^2_{\rm SB}} (\widetilde{q} - \widetilde{q}^\ell_{\rm ar})^2\} \\ \times \frac{1}{(s_{\rm SB} \sqrt{2\pi})^{n_w}} \exp\{-\frac{1}{2 s^2_{\rm SB}} \|\widetilde{\mathbf{w}} - \widetilde{\mathbf{w}}^\ell_{\rm ar}\|^2\} \, , \tag{14}$$

in which $s_{\rm SB}$ is the following Silverman bandwidth, $s_{\rm SB} = (4/(N_{\rm ar}(3 + n_w)))^{1/(5+n_w)}$, and where, for $\ell = 1, \ldots, N_{\rm ar}$, $\widetilde{q}^\ell_{\rm ar} = (q^\ell_{\rm ar} - \underline{q})/\sigma_Q$ and for $i = 1, \ldots, n_w$, $\widetilde{w}^\ell_{{\rm ar},i} = (w^\ell_{{\rm ar},i} - \underline{w}_i)/\sigma_i$. From Eqs. (12), (13),and (14), it can be deduced that

$$E\{\widetilde{Q} \,|\, \widetilde{\mathbf{W}} = \widetilde{\mathbf{w}}^0\} = \frac{\sum_{\ell=1}^{N_{\rm ar}} \widetilde{q}^\ell_{\rm ar} \, \exp\{-\frac{1}{2 s^2_{\rm SB}} \|\widetilde{\mathbf{w}}^0 - \widetilde{\mathbf{w}}^\ell_{\rm ar}\|^2\}}{\sum_{\ell=1}^{N_{\rm ar}} \exp\{-\frac{1}{2 s^2_{\rm SB}} \|\widetilde{\mathbf{w}}^0 - \widetilde{\mathbf{w}}^\ell_{\rm ar}\|^2\}} \, , \tag{15}$$

$$q^{\rm ML}(\mathbf{w}_0) = \arg\max_{\widetilde{q}} \sum_{\ell=1}^{N_{\rm ar}} \exp\{-\frac{1}{2 s^2_{\rm SB}} ((\widetilde{q} - \widetilde{q}^\ell_{\rm ar})^2 + \|\widetilde{\mathbf{w}}^0 - \widetilde{\mathbf{w}}^\ell_{\rm ar}\|^2)\} \, . \tag{16}$$

6.3. Choice of the optimization algorithm

For each value $\mathbf{w}^0$ proposed by the optimization algorithm, the evaluation of the cost function is performed using PLoM as we have explained in Sections 6.1 and 6.2. Nevertheless, an algorithm has to be chosen for solving the optimization problem defined either by Eq. (6) with Eqs. (7) and (8) or by Eq. (6) with Eqs. (10) and (9). Note that in the application of Section 7, we will consider the optimization problem defined by the second set of equations. The optimization algorithms have extensively been developed for several decades and are today really efficient (see for instance [98] for problems in a deterministic framework). Concerning the algorithms for solving optimization problems in a statistical framework, many methods have been proposed such as the gradient-based learning that is adapted to convex problems [99, 100], the global search algorithms such as the stochastic algorithms, the genetic algorithm, and the evolutionary algorithms [101, 102]. If dimension n_w is small, a grid search algorithm can also be used (see the numerical application presented in Section 7).

6.4. Optimization strategy

We assume here that the optimization problem defined by Eq. (6) with Eqs. (10) and (9) is considered (which will be the case in Section 7). Once the optimal control parameter $\mathbf{w}^{\text{opt}}$ is found from solving this optimization problem, the HDM is rerun once, using the control parameter $\mathbf{w}^{\text{opt}}$. We then introduce an error function $e_{\text{dB,k}}$ associated with observation number k, which is given, using the trapezoidal rule, by:

$$e_{\text{dB,k}}(\mathbf{w}) = \left(\frac{1}{2(n_\omega - 1)} \sum_{m=1}^{n_\omega - 1} \left(f_{m+1}^k(\mathbf{w}) + f_m^k(\mathbf{w}) \right) \right)^{1/2} , \tag{17}$$

in which $f_m^k(\mathbf{w}) = \left([q(\mathbf{w})]_{mk} - q_m^{\text{targ}} \right)^2$. The error $e_{\text{dB,n}_\text{o}}(\mathbf{w}^{\text{opt}})$ characterizes the quality of the model updating with respect to the target. It is recalled that the cost function in Eq. (6) relies on the estimation of the conditional statistics using PLoM. The PLoM method is used for generating $N_{\text{ar}} = n_{\text{MC}} \times N_d$ realizations based on N_d calls to the HDM (see Appendix A) in which n_{MC} is an integer greater than 1. It should be noted that increasing N_d may not lead to an improved updating because of the lack of monotonicity in N_d of the error function defined by Eq. (17) (as mentioned in Section 1 (iii)). The global strategy is then to solve the optimization problem several times by considering subsets of the training set (the PLoM method being used for each subset), because a subset can potentially yield a better updating than the training set (due to the lack of monotonicity). For each optimization problem related to a given subset, we estimate the optimal value $\mathbf{w}^{\text{opt}}$ of $\mathbf{w}$ and one call to the HDM with $\mathbf{w} = \mathbf{w}^{\text{opt}}$ is then required for estimating the error defined by Eq. (17). Let N_c be the maximum number of calls to the HDM that we can afford. A number $N_d < N_c$ of calls to the HDM are done to obtain the training set. Let $N_{cd} = N_c - N_d$ be the number of calls to the HDM that are left. This means that N_{cd} optimization problems (with associated PLoM computation) can be carried out for improving the updating.

7. Numerical application

The mechanical system considered in this application has been voluntarily chosen as a simple one and is comprehensively described so that the results presented can be reproduced.

7.1. Defining the computational model

As a numerical application, a structure made up of plates in bending mode is considered, see Fig. 2. It is constituted of two structural levels, such that it exhibits both global and local

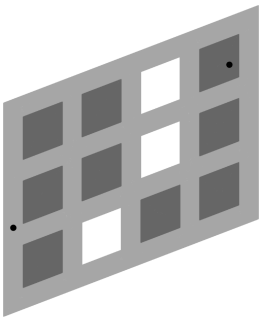

Figure 2: Multiscale plate structure including the position of the input and output nodes of the considered FRF (big black dots)

structural elastic modes. This structure is similar to the one analyzed in [103] in which global and local modes are plotted. This way, despite its simplicity, the structure presents similar characteristics as the structures of interest as described in Section 1. The structure is rectangular with length 0.26 m (x axis) and width 0.2 m (z axis), and it includes twelve square slots with dimension 0.04 m, three of them being empty (holes) and nine of them being thin panels. These twelve slots are regularly spaced, such that the matrix frame (or frame) is of width 0.02 m. The structure is modeled using isotropic Kirchhoff plate elements. The nominal properties of the structure are now given. The plate thickness h_1 of the frame is of $h_1 = 2 \times 10^{-3}$ m, its Young modulus is $E_1 = 210 \times 10^9$ GPa, its Poisson ratio is $\nu_1 = 0.3$, and its mass density is $\rho_1 = 2600$ kg/m^3. For the nine panels, the Young modulus is $E_2 = 5 \times 10^9$ GPa, the Poisson ratio is $\nu_2 = 0.3$, and the mass density is $\rho_2 = 5200$ kg/m^3. Regarding their thickness, it is $h_2 = 1.1 \times 10^{-4}$ m for the bottom-left, bottom-right, and top-mid panels, whereas it is $h_2' = 9 \times 10^{-5}$ m for the six remaining panels. As boundary conditions, the four corners are fixed. The finite element model has $n_u = 163{,}032$ dof. The quantity of interest is the FRF between the transverse displacement dof of the two nodes depicted in Fig. 2. Taking the bottom left corner as origin, the coordinates (m) of the two nodes are $(x_1 = 0.01, z_1 = 0.08)$ and $(x_2 = 0.23, z_2 = 0.155)$. We then have $n_o = 1$. The FRF is uniformly sampled using $n_\omega = 5000$ frequency points.

7.2. Defining the probabilistic model of the control parameter $\mathbf{W}$

The computational model depends on a control parameter $\mathbf{w} = (w_1, \ldots, w_{n_w})$ with dimension $n_w = 4$. Let $k_1 = E_1/(3(1-2\nu_1))$, $g_1 = E_1/(2(1+\nu_1))$, $k_2 = E_2/(3(1-2\nu_2))$, and $g_2 = E_2/(2(1+\nu_2))$ denote the bulk and shear moduli of the frame and of the panels, respectively. The $n_w = 4$ components of the control parameter $\mathbf{w}$ are given by $w_1 = Log(k_1)$, $w_2 = Log(g_1)$, $w_3 = Log(k_2)$, and $w_4 = Log(g_2)$. The $\mathbb{R}^{n_w}$-valued random variable $\mathbf{W} = (W_1, \ldots, W_{n_w})$ associated with $\mathbf{w}$ is defined as follows.

- Let K_1 denote the random bulk modulus of the frame. Its mean value is k_1 and its coefficient of variation is denoted as δ_{K_1}. The probability distribution of K_1 is chosen as a

Gamma distribution with shape parameter $\alpha_{K_1} = \delta_{K_1}^{-1/2}$ and rate parameter $\beta_{K_1} = \alpha_{K_1}/k_1$. Random variable W_1 is given by $W_1 = Log(K_1)$.

- Similarly, let G_1 denote the random shear modulus of the frame. Its mean value is g_1 and its coefficient of variation is denoted as δ_{G_1}. Random variable G_1 follows a Gamma distribution with shape parameter $\alpha_{G_1} = \delta_{G_1}^{-1/2}$ and rate parameter $\beta_{G_1} = \alpha_{G_1}/g_1$. Random variable W_2 is given by $W_2 = Log(G_1)$.

- Let K_2 denote the random bulk modulus of the panels. Its mean value is k_2 and its coefficient of variation is denoted as δ_{K_2}. The probability distribution of K_2 is chosen as a Gamma distribution with shape parameter $\alpha_{K_2} = \delta_{K_2}^{-1/2}$ and rate parameter $\beta_{K_2} = \alpha_{K_2}/k_2$. Random variable W_3 is given by $W_3 = Log(K_2)$.

- Similarly, let G_2 denote the random shear modulus of the panels. Its mean value is g_2 and its coefficient of variation is denoted as δ_{G_2}. Random variable G_2 follows a Gamma distribution with shape parameter $\alpha_{G_2} = \delta_{G_2}^{-1/2}$ and rate parameter $\beta_{G_2} = \alpha_{G_2}/g_2$. Random variable W_4 is given by $W_4 = Log(G_2)$.

7.3. Parameterized reduced-order computational model and training set computation

The training set is obtained based on the realizations of random control parameter $\mathbf{W}$. The admissible set $C_{\mathbf{W}}$ of $\mathbf{W}$ is such that $k_1 \in]0, +\infty]$, $k_2 \in]0, +\infty]$, $\nu_1 \in]0.15\,, 0.45]$, and $\nu_2 \in]0.15\,, 0.45]$. For each material, according to the paper [104], the bulk and shear moduli are statistically independent and it is shown that we have:

$$\delta_{G_1} = \frac{1}{\sqrt{-4 + 5/\delta_{K_1}}}\,, \tag{18}$$

$$\delta_{G_2} = \frac{1}{\sqrt{-4 + 5/\delta_{K_2}}}\,. \tag{19}$$

In addition, it is assumed that the random mechanical properties are independent from one material to the other. For the training set, we choose $\delta_{K_1} = 0.15$ and $\delta_{K_2} = 0.5$. This means that the material variability is greater for the panels than for the main frame. The nominal values given in Section 7.1 are used and allow to obtain the random realizations of $\mathbf{W}$ through the steps detailed in Section 7.2. As explained in Section 1, for the case of an HDM, the number N_c of calls to the computational model is limited by the computational resources. In this application, we then also choose a small value $N_c = 200$ of the maximum number of calls to the HDM. The training set is then generated by $N_d = 175$ independent realizations of $\mathbf{W}$. The value of N_d has been chosen to let 12 optimization problems to be solved with and without PLoM ($2 \times 13 + 175 = 201 \sim 200$). For a fixed realization of $\mathbf{W}$, the computational model is used for computing the corresponding realization of the FRF. As explained in Section 4, this involves computing all the structural elastic modes up to a given cutoff frequency, for which the number of elastic modes is determined by using the LDL factorization. The FRF is computed for $n_\omega = 5000$ uniformly sampled frequencies in $\Omega = 2\pi\times]0, 1000]$ rad/s. In order to get a good convergence of the modal representation for all the values of the control parameter considered in the training set, a cutoff frequency of 1500 Hz is considered. A modal damping model is used with the same damping ratio $\xi = 0.01$.

7.4. Remark concerning the representativeness of the presented example

The following comments can be done concerning the representativeness of the presented example with respect to the nuclear engineering (NE) application mentioned in Section 1. Regarding the elastic modes, in the present application, there are significantly less (a few hundreds). Nevertheless, for both cases, the elastic modes include a relatively small number of global modes, which are preponderant in the structural response. This means that for both cases, the influence of local modes is rather diffuse and sometimes imperceptible for one given mode. The frequency content of the structural response is not that much more complex for the case of the NE application as for the case of the present application. Regarding the low number of parameters used (here four) compared to NE applications, for which there would be, for example, a hundred parameters, the proposed methodology would remain the same. Between the two cases, the difference would be the choice of the optimization algorithm. In either case, the number of evaluations of the cost function would be too large. We therefore need a surrogate model, which we proposed by building a statistical surrogate model using PLoM. Regarding the under-observability of the model, only one FRF is observed (only one target FRF) and for this FRF, only one "experimental" realization is considered available. This is a highly under-observed case and for the NE application, the under-observability is slightly less because several FRF are observed at several locations of the outer shell.

7.5. Model updating

In this Section, two cases are presented, corresponding to two different choices of target FRF.

Case 1. For this case, we consider a target FRF generated by the computational model with $E_1^{\text{target}} = 238.7$ GPa, $\nu_1^{\text{target}} = 0.248$, $E_2^{\text{target}} = 3.7$ GPa, and $\nu_2^{\text{target}} = 0.351$. We consider a sampling of N_d up to 175, such that $N_d \in \mathcal{S}_{N_d} = \{25, 38, 50, 63, 75, 88, 100, 113, 125, 138, 150, 163, 175\}$. For fixed N_d, we define n_{MC} such that $N_{\text{ar}} = n_{\text{MC}} \times N_d$ is the closest to 20,000. For fixed (N_d, n_{MC}) couple with $N_d \in \mathcal{S}_{N_d}$, the PLoM method is used to generate $N_{\text{ar}} = n_{\text{MC}} \times N_d$ learned realizations, based on which the optimization problem defined by Eqs. (6), (10), and (9) is solved and yields $\mathbf{w}^{\text{opt}}$ that is used to update the computational model and obtain the updated FRF (as explained in Section 6.4). Concerning the PLoM parameters used in the algorithm summarized in Appendix Appendix A, the value of ε_{PCA} is fixed to 10^{-3}. For the 13 values of N_d belonging to $\mathcal{S}_{N_d}$, which vary from 25 to 175, the reduced-order dimension ν of the PCA varies from 22 to 82, the optimal value m_{opt} of the truncated diffusion-maps basis is given by $m_{\text{opt}} = \nu + 1$, and the optimal value ε_{opt} varies from 40 to 204. As an illustration, for $N_d = 175$, for which $\nu = 82$, $m_{\text{opt}} = 83$, and $\varepsilon_{\text{opt}} = 204$, Fig. 3 displays the distribution of the eigenvalues μ_α of the PCA of $\mathbf{X}$ and Fig. 4 displays the distribution of the eigenvalues λ_α of the transition matrix. Regarding the optimization algorithm, a grid search is performed, with 35 points per axis (there are four axes, for E_1, ν_1, E_2, and ν_2). The updated FRF is compared to the target FRF using the error defined by Eq. (17). In parallel, the exact same procedure is also carried out using the training set instead of the learned set. The total number of additional calls to the computational model is twice the size of set $\mathcal{S}_{N_d}$, that is 26, which makes it a total of 201 calls to the computational model. It can be seen in Fig. 5 that the updating is best for $N_d = 125$ using the learned set. The error is of 3.4 dB and the updated parameters are $E_1^{\text{opt}} = 239.4$ GPa, $\nu_1^{\text{opt}} = 0.278$, $E_2^{\text{opt}} = 3.6$ GPa, and $\nu_2^{\text{opt}} = 0.374$. The quality of the updated model is put into evidence in Fig. 6 where the nominal FRF, the target FRF, and the updated FRF using the learned set with $N_d = 125$ and $N_{\text{ar}} = 20{,}000$ are depicted. It can be seen that the proposed methodology is successful in updating the computational model.

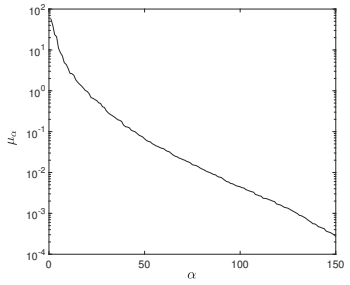

Figure 3: For $N_d = 175$, $\nu = 82$, $m_{\text{opt}} = 83$, and $\varepsilon_{\text{opt}} = 204$, distribution of the eigenvalues μ_α of the PCA of $\mathbf{X}$.

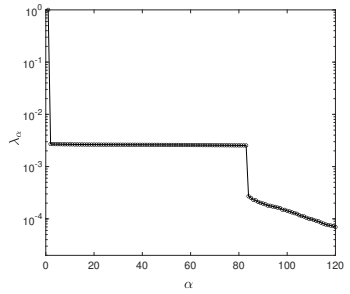

Figure 4: For $N_d = 175$, $\nu = 82$, $m_{\text{opt}} = 83$, and $\varepsilon_{\text{opt}} = 204$, distribution of the eigenvalues λ_α of the transition matrix in $\log_{10}$ scale.

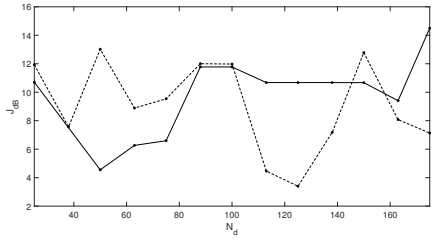

Figure 5: Case 1: for each value of N_d belonging to $\mathcal{S}_{N_d}$, value of the error obtained using the learned set with $N_{\text{ar}} = N_d \times n_{\text{MC}} \sim 20\,000$ realizations (dashed line) and using the training set with N_d realizations (solid line)

Case 2. For this case, we consider a target FRF generated with the computational model with $E_1^{\text{target}} = 254$ GPa, $\nu_1^{\text{target}} = 0.312$, $E_2^{\text{target}} = 5.8$ GPa, and $\nu_2^{\text{target}} = 0.273$. The entire procedure is kept identical and the results are shown in Figs. 7 and 8. It can be seen in Fig. 7 that the updating is best for $N_d = 138$ using the training set (the fact that the training set yields a better optimum than the learned set is discussed in Section 7.6 as a complement to the reasons already given in Section 1-(iii)). The error is of 2.2 dB and the updated parameters are $E_1^{\text{opt}} = 249.9$ GPa, $\nu_1^{\text{opt}} = 0.328$, $E_2^{\text{opt}} = 5.4$ GPa, and $\nu_2^{\text{opt}} = 0.358$. The quality of the updated model is put into

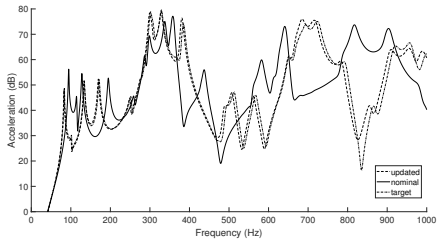

Figure 6: Comparison between the nominal FRF (solid line), the target FRF (dash-dotted line), and the updated FRF (dashed line)

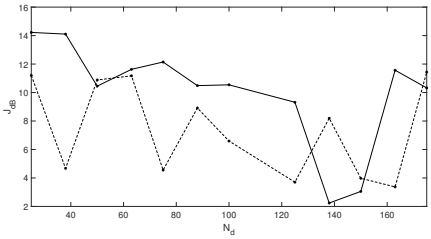

Figure 7: Case 2: for each value of N_d belonging to $\mathcal{S}_{N_d}$, value of the error obtained using the learned set with $N_{\text{ar}} = N_d \times n_{\text{MC}} \sim 20\,000$ realizations (dashed line) and using the training set with N_d realizations (solid line)

evidence in Fig. 8 where the nominal FRF, the target FRF, and the updated FRF using the training set with $N_d = 138$ are depicted. It can be seen that the proposed methodology is successful in updating the computational model.

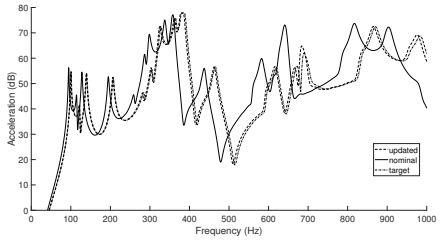

Figure 8: Comparison between the nominal FRF (solid line), the target FRF (dash-dotted line), and the updated FRF (dashed line)

7.6. Discussion on the results presented

First, we recall the framework of the proposed updating methodology based on a single target FRF. For a given large computational model, only N_d realizations can be computed, with N_d having a small value. In this context, the objective is to improve the computational model using the single target FRF. So, the metholodogy that we have proposed is the following. For such a

given value of N_d, the training set and a learned set are generated. The optimization problem is solved on the one hand with the training set and on the other hand with the learned set. For this fixed value of N_d, the best updated model is the one having the smallest error between the target FRF and the updated FRF (error defined by Eq. (17)). In this framework of the use of the methodology, the notion of convergence with respect to N_d has no meaning. Figures 5 and 7 effectively show that the error has large fluctuations as a function of N_d. Such fluctuations are due to the small value of N_d (the largest is 175), to the fact that only a single target FRF is available, that there are multiple control parameters, and that the optimization problem is nonconvex. Consequently, there is no uniqueness of the optimal control parameters. Clearly, if the training set could be constructed for a very large value N_d^* of N_d, the error could perhaps, in this case, decrease for $N_d > N_d^*$. For instance, for the application presented, the updating has also been performed using the training set with $N_d = 2000$ without obtaining a clear convergence of the error, and the available computing resources did not permit to consider an even greater value of N_d.

8. Conclusions

We have presented a formulation and a methodology for the updating of high-dimensional computational models with uncertainties of complex structures, which present an enormous number of global modes and local modes in the frequency band of analysis. The model updating is performed in an under-observed framework for which only one experimental frequency response function is available. The methodology we have proposed is based on the introduction of a parameterized ROM and on the use of a probabilistic learning algorithm, the PLoM that has been developed to deal with small data cases, and which allows to solve the optimization problem without using the resolution of the HDM for which a single evaluation is very expensive. The methodology presented has been validated on a representative example from the point of view of the difficulties encountered for the dynamic systems described in the introduction. Obviously the structure considered in the example presented is much simpler than those of the targeted applications, but this choice was made so that the results presented can be reproduced. Finally, as the example presented is really simple, a multi-frequency model reduction with or without substructuring techniques is not necessary for constructing the parameterized ROM. This allowed us to simplify the presentation of the methodology while remaining to the essentials. However, these methodological additions can be implemented without difficulty in the proposed method. We refer the reader to Section 7.6 for the discussion about the framework of the use of the proposed method.

Appendix A. Summary of the probabilistic learning on manifolds (PLoM) algorithm and its parameterization

The PLoM approach [70, 71, 92], which has specifically been developed for small data (in opposite to big data) starts from a training set $\mathcal{D}_d$ made up of a relatively small number N_d of points. It is assumed that $\mathcal{D}_d$ is generated with an underlying stochastic manifold related to a $\mathbb{R}^n$-valued random variable $\mathbf{X} = (\mathbf{Q}, \mathbf{W})$, defined on a probability space $(\Theta, \mathcal{T}, \mathcal{P})$, in which $\mathbf{Q}$ is the quantity of interest that is a $\mathbb{R}^{n_q}$-random variable, where $\mathbf{W}$ is the control parameter that is a $\mathbb{R}^{n_w}$-random variable, and where $n = n_q + n_w$. Another $\mathbb{R}^{m_u}$- valued random variable $\mathbf{U}$ defined on $(\Theta, \mathcal{T}, \mathcal{P})$ can also be considered, which is an uncontrolled parameter and/or a noise. Random

variable $\mathbf{Q}$ is assumed to be written as $\mathbf{Q} = \mathbf{f}(\mathbf{U}, \mathbf{W})$ in which the measurable mapping $\mathbf{f}$ is not explicitly known. The joint probability distribution $P_{\mathbf{W},\mathbf{U}}(d\mathbf{w}, d\mathbf{u})$ of $\mathbf{W}$ and $\mathbf{U}$ is assumed to be given. Note that in this paper, we have not considered any uncontrolled variable. The non-Gaussian probability measure $P_{\mathbf{X}}(\mathbf{x}) = P_{\mathbf{Q},\mathbf{W}}(d\mathbf{q}, d\mathbf{w})$ of $\mathbf{X} = (\mathbf{Q}, \mathbf{W})$ is concentrated in a region of $\mathbb{R}^n$ for which the only available information is the cloud of the points of training set $\mathcal{D}_d$. The PLoM method makes it possible to generate the learned set $\mathcal{D}_{\text{ar}}$ for $\mathbf{X}$ whose $n_{\text{MC}} \gg N_d$ points (learned realizations) are generated by the non-Gaussian probability measure that is estimated using the training set. The concentration of the probability measure is preserved thanks to the use of a diffusion-maps basis that allows to enrich the available information from the training set. Using the learned set $\mathcal{D}_{\text{ar}}$, PLoM allows for carrying out any conditional statistics such as $\mathbf{w} \mapsto E\{\mathbf{Q}|\mathbf{W} = \mathbf{w}\}$ from C_w in $\mathbb{R}^{n_q}$, and consequently, to directly construct metamodels in a probabilistic framework.

The training set $\mathcal{D}_d$ is made up of the N_d independent realizations $\mathbf{x}_d^j = (\mathbf{q}_d^j, \mathbf{w}_d^j)$ in $\mathbb{R}^n = \mathbb{R}^{n_q} \times \mathbb{R}^{n_w}$ for $j \in \{1, \ldots, N_d\}$ of random variable $\mathbf{X} = (\mathbf{Q}, \mathbf{W})$. The PLoM method allows for generating the learned set $\mathcal{D}_{\text{ar}}$ made up of $N_{\text{ar}} \gg N_d$ learned realizations $\{\mathbf{x}_{\text{ar}}^\ell, \ell = 1, \ldots, N_{\text{ar}}\}$ of random vector $\mathbf{X}$. As soon as the learned set has been constructed, the learned realizations for $\mathbf{Q}$ and $\mathbf{W}$ can be extracted as $(\mathbf{q}_{\text{ar}}^\ell, \mathbf{w}_{\text{ar}}^\ell) = \mathbf{x}_{\text{ar}}^\ell$ for $\ell = 1, \ldots, N_{\text{ar}}$.

(A.1) Reduced representation. The N_d independent realizations $\{\mathbf{x}_d^j, j = 1, \ldots, N_d\}$ are represented by the matrix $[x_d] = [\mathbf{x}_d^1 \ldots \mathbf{x}_d^{N_d}]$ in $\mathbb{M}_{n,N_d}$. Let $[\mathbf{X}] = [\mathbf{X}^1, \ldots, \mathbf{X}^{N_d}]$ be the random matrix with values in $\mathbb{M}_{n,N_d}$, whose columns are N_d independent copies of random vector $\mathbf{X}$. Using the PCA of $\mathbf{X}$, random matrix $[\mathbf{X}]$ is written as,

$$[\mathbf{X}] = [\underline{x}] + [\varphi]\,[\mu]^{1/2}\,[\mathbf{H}]\,, \tag{A.1}$$

in which $[\mathbf{H}] = [\mathbf{H}^1, \ldots, \mathbf{H}^{N_d}]$ is a $\mathbb{M}_{\nu,N_d}$-valued random matrix, where $\nu \leq n$, and where $[\mu]$ is the $(\nu \times \nu)$ diagonal matrix of the ν positive eigenvalues of the empirical estimate of the covariance matrix of $\mathbf{X}$. The $(n \times \nu)$ matrix $[\varphi]$ is made up of the associated eigenvectors such $[\varphi]^T\,[\varphi] = [I_\nu]$. The matrix $[\underline{x}]$ in $\mathbb{M}_{n,N_d}$ has identical columns, each one being equal to the empirical estimate $\underline{\mathbf{x}} \in \mathbb{R}^n$ of the mean value of random vector $\mathbf{X}$. The columns of $[\mathbf{H}]$ are N_d independent copies of a random vector $\mathbf{H}$ with values in $\mathbb{R}^\nu$. The realization $[\eta_d] = [\boldsymbol{\eta}_d^1 \ldots \boldsymbol{\eta}_d^{N_d}] \in \mathbb{M}_{\nu,N_d}$ of $[\mathbf{H}]$ is computed by $[\eta_d] = [\mu]^{-1/2}[\varphi]^T\,([x_d] - [\underline{x}])$. The value ν is classically calculated in order that the L^2- error function $\nu \mapsto \text{err}_{\mathbf{X}}(\nu)$ defined by

$$\text{err}_{\mathbf{X}}(\nu) = 1 - \frac{\sum_{\alpha=1}^{\nu} \mu_\alpha}{E\{\|\mathbf{X}\|^2\}}\,, \tag{A.2}$$

be smaller than ε_{PCA}. If $\nu < n$, then there is a statistical reduction.

(A.2) Construction of a reduced-order diffusion-maps basis. For preserving the concentration of the learned realizations in the region in which the points of the training set are concentrated, the PLoM relies on the diffusion-maps method [105, 106]. This is an algebraic basis of vector space $\mathbb{R}^{N_d}$, which is constructed using the diffusion maps. Let $[K]$ and $[b]$ be the matrices such that, for all i and j in $\{1, \ldots, N_d\}$, $[K]_{ij} = \exp\{-(4\,\varepsilon_{\text{DM}})^{-1}\|\boldsymbol{\eta}_d^i - \boldsymbol{\eta}_d^j\|^2\}$ and $[b]_{ij} = \delta_{ij}\,b_i$ with $b_i = \sum_{j=1}^{N_d}[K]_{ij}$, in which $\varepsilon_{\text{DM}} > 0$ is a smoothing parameter. The eigenvalues $\lambda_1, \ldots, \lambda_{N_d}$ and the associated eigenvectors $\boldsymbol{\psi}^1, \ldots, \boldsymbol{\psi}^{N_d}$ of the right-eigenvalue problem $[\mathbb{P}]\,\boldsymbol{\psi}^\alpha = \lambda_\alpha\,\boldsymbol{\psi}^\alpha$ are such that $1 = \lambda_1 > \lambda_2 \geq \ldots \geq \lambda_{N_d}$ and are computed by solving the generalized eigenvalue problem $[K]\,\boldsymbol{\psi}^\alpha =$

$\lambda_\alpha\,[b]\,\boldsymbol{\psi}^\alpha$ with the normalization $<[b]\,\boldsymbol{\psi}^\alpha, \boldsymbol{\psi}^\beta>= \delta_{\alpha\beta}$. The eigenvector $\boldsymbol{\psi}^1$ associated with $\lambda_1 = 1$ is a constant vector. For a given integer $\kappa \geq 0$, the diffusion-maps basis $\{\mathbf{g}^1, \ldots, \mathbf{g}^\alpha, \ldots, \mathbf{g}^{N_d}\}$ is a vector basis of $\mathbb{R}^{N_d}$ defined by $\mathbf{g}^\alpha = \lambda_\alpha^\kappa\, \boldsymbol{\psi}^\alpha$. For a given integer m, the reduced-order diffusion-maps basis of order m is defined as the family $\{\mathbf{g}^1, \ldots, \mathbf{g}^m\}$ that is represented by the matrix $[g_m] = [\mathbf{g}^1 \ldots \mathbf{g}^m] \in \mathbb{M}_{N_d,m}$ with $\mathbf{g}^\alpha = (g_1^\alpha, \ldots, g_{N_d}^\alpha)$ and $[g_m]_{\ell\alpha} = g_\ell^\alpha$. This basis depends on two parameters, ε_{DM} and m, which have to be identified. It is proven in [71], that the PLoM method does not depend on κ that can therefore be chosen to 0.

We have to find the optimal value $m_{\text{opt}} \leq N_d$ of m and the smallest value $\varepsilon_{\text{opt}} > 0$ of ε_{DM} such that (see [72])

$$1 = \lambda_1 > \lambda_2(\varepsilon_{\text{opt}}) \simeq \ldots \simeq \lambda_{m_{\text{opt}}}(\varepsilon_{\text{opt}}) \gg \lambda_{m_{\text{opt}}+1}(\varepsilon_{\text{opt}}) \geq \ldots \geq \lambda_{N_d}(\varepsilon_{\text{opt}}) > 0\,, \tag{A.3}$$

with an amplitude jump equal to an order of magnitude (a factor 10 as demonstrated in [71]) between $\lambda_{m_{\text{opt}}}(\varepsilon_{\text{opt}})$ and $\lambda_{m_{\text{opt}}+1}(\varepsilon_{\text{opt}})$. A further in-depth analysis makes it possible to state the following algorithm to estimate ε_{opt} and m_{opt}. Let $\varepsilon_{\text{DM}} \mapsto \text{Jump}(\varepsilon_{\text{DM}})$ be the function on $]0, +\infty[$ defined by

$$\text{Jump}(\varepsilon_{\text{DM}}) = \lambda_{m_{\text{opt}}+1}(\varepsilon_{\text{DM}})/\lambda_2(\varepsilon_{\text{DM}})\,. \tag{A.4}$$

The algorithm is the following:
- set the value of m to $m_{\text{opt}} = \nu + 1$;
- identify the smallest possible value ε_{opt} of ε_{DM} in order that $\text{Jump}(\varepsilon_{\text{opt}}) \leq 0.1$ and such that Equation (A.3) be verified.

(A.3) Reduced-order representation of random matrices $[\boldsymbol{H}]$ *and* $[\boldsymbol{X}]$. The diffusion-maps vectors $\mathbf{g}^1, \ldots, \mathbf{g}^m \in \mathbb{R}^{N_d}$ span a subspace of $\mathbb{R}^{N_d}$ that characterizes, for the optimal values m_{opt} and ε_{opt} of m and ε_{DM}, the local geometry structure of data set $\{\boldsymbol{\eta}_d^j, j = 1, \ldots, N_d\}$. So the PLoM method introduces the $\mathbb{M}_{\nu,N_d}$-valued random matrix $[\mathbf{H}_m] = [\mathbf{Z}_m]\,[g_m]^T$ with $m \leq N_d$, corresponding to a data-reduction representation of random matrix $[\mathbf{H}]$, in which $[\mathbf{Z}_m]$ is a $\mathbb{M}_{\nu,m}$-valued random matrix. The MCMC generator of random matrix $[\mathbf{Z}_m]$ belongs to the class of Hamiltonian Monte Carlo methods, is explicitly described in [70], and is mathematically detailed in Theorem 6.3 of [71]. For generating the learned set, the best probability measure of $[\mathbf{H}_m]$ is obtained for $m = m_{\text{opt}}$ and using the previously defined $[g_{m_{\text{opt}}}]$. For these optimal quantities m_{opt} and $[g_{m_{\text{opt}}}]$, the generator allows for computing n_{MC} realizations $\{[\mathbf{z}_{\text{ar}}^\ell], \ell = 1, \ldots, n_{\text{MC}}\}$ of $[\mathbf{Z}_{m_{\text{opt}}}]$ and therefore, for deducing the n_{MC} realizations $\{[\boldsymbol{\eta}_{\text{ar}}^\ell], \ell = 1, \ldots, n_{\text{MC}}\}$ of $[\mathbf{H}_{m_{\text{opt}}}]$. The reshaping of matrix $[\boldsymbol{\eta}_{\text{ar}}^\ell] \in \mathbb{M}_{\nu,N_d}$ allows for obtaining $N_{\text{ar}} = n_{\text{MC}} \times N_d$ learned realizations $\{\boldsymbol{\eta}_{\text{ar}}^{\ell'}, \ell' = 1, \ldots, N_{\text{ar}}\}$ of $\mathbf{H}$. These learned realizations allow for estimating converged statistics on $\mathbf{H}$ and then on $\mathbf{X}$, such as pdf, moments, or conditional expectation of the type $E\{\boldsymbol{\xi}(\mathbf{Q})\,|\,\mathbf{W} = \mathbf{w}\}$ for $\mathbf{w}$ given in $\mathbb{R}^{n_w}$ and for any given vector-valued function $\boldsymbol{\xi}$ defined on $\mathbb{R}^{n_q}$.

(A.4) Criterion for quantifying the concentration of the probability measure of random matrix $[\boldsymbol{H}_{m_{\text{opt}}}]$. For $m \leq N_d$, the concentration of the probability measure of random matrix $[\mathbf{H}_m]$ is defined (see [71]) by

$$d_{N_d}^2(m) = E\{\|[\mathbf{H}_m] - [\eta_d]\|^2\}/\|[\eta_d]\|^2\,. \tag{A.5}$$

Let $\mathcal{M}_{\text{opt}} = \{m_{\text{opt}}, m_{\text{opt}} + 1, \ldots, N_d\}$ in which m_{opt} is the optimal value of m previously defined. Theorem 7.8 of [71] shows that $\min_{m \in \mathcal{M}_{\text{opt}}} d_{N_d}^2(m) \leq 1 + m_{\text{opt}}/(N_d - 1) < d_{N_d}^2(N_d)$, which means that the PLoM method, for $m = m_{\text{opt}}$ and $[g_{m_{\text{opt}}}]$ is a better method than the usual one corresponding to $d_{N_d}^2(N_d) = 1 + N_d/(N_d - 1) \simeq 2$. Using the n_{MC} realizations $\{[\boldsymbol{\eta}_{\text{ar}}^\ell], \ell = 1, \ldots, n_{\text{MC}}\}$ of

$[\mathbf{H}_{m_{\rm opt}}]$, we have the estimate $d^2_{N_d}(m_{\rm opt}) \simeq (1/n_{\rm MC}) \sum_{\ell=1}^{n_{\rm MC}} \{\|[\boldsymbol{\eta}^{\ell}_{\rm ar}] - [\eta_d]\|^2\} / \|[\eta_d]\|^2$.

(A.5) Generation of learned realizations $\{\boldsymbol{\eta}^{\ell'}_{\rm ar}, \ell' = 1, \ldots, N_{\rm ar}\}$ *of random vector* $\boldsymbol{H}$. The MCMC generator is detailed in [70]. Let $\{([\boldsymbol{\mathcal{Z}}(t)], [\boldsymbol{\mathcal{Y}}(t)]), t \in \mathbb{R}^+\}$ be the unique asymptotic (for $t \to +\infty$) stationary diffusion stochastic process with values in $\mathbb{M}_{\nu,m_{\rm opt}} \times \mathbb{M}_{\nu,m_{\rm opt}}$, of the following reduced-order ISDE (stochastic nonlinear second-order dissipative Hamiltonian dynamic system), for $t > 0$,

$$
\begin{aligned}
d[\boldsymbol{\mathcal{Z}}(t)] &= [\boldsymbol{\mathcal{Y}}(t)]\, dt\,, \\
d[\boldsymbol{\mathcal{Y}}(t)] &= [\mathcal{L}([\boldsymbol{\mathcal{Z}}(t)])]\, dt - \frac{1}{2} f_0\, [\boldsymbol{\mathcal{Y}}(t)]\, dt \\
&\quad + \sqrt{f_0}\, [d\boldsymbol{\mathcal{W}}^{\rm wien}(t)]\,,
\end{aligned}
$$

with $[\boldsymbol{\mathcal{Z}}(0)] = [\eta_d]\,[a]$ and $[\boldsymbol{\mathcal{Y}}(0)] = [\boldsymbol{\mathcal{N}}]\,[a]$, in which

$$
[a] = [g_{m_{\rm opt}}]\, ([g_{m_{\rm opt}}]^T\, [g_{m_{\rm opt}}])^{-1} \in \mathbb{M}_{N_d, m_o pt}\,.
$$

(1) $[\mathcal{L}([\boldsymbol{\mathcal{Z}}(t)])] = [L([\boldsymbol{\mathcal{Z}}(t)]\,[g_{m_{\rm opt}}]^T)]\,[a]$ is a random matrix with values in $\mathbb{M}_{\nu,m_{\rm opt}}$. For all $[u] = [\mathbf{u}^1 \ldots \mathbf{u}^{N_d}]$ in $\mathbb{M}_{\nu,N_d}$ with $\mathbf{u}^j = (u^j_1, \ldots, u^j_\nu)$ in $\mathbb{R}^\nu$, the matrix $[L([u])]$ in $\mathbb{M}_{\nu,N_d}$ is defined, for all $k = 1, \ldots, \nu$ and for all $j = 1, \ldots, N_d$, by

$$
\begin{aligned}
[L([u])]_{kj} &= \frac{1}{p(\mathbf{u}^j)}\, \{\boldsymbol{\nabla}_{\mathbf{u}^j}\, p(\mathbf{u}^j)\}_k\,, \qquad \text{(A.6)} \\
p(\mathbf{u}^j) &= \frac{1}{N_d} \sum_{j'=1}^{N_d} \exp\{-\frac{1}{2\widehat{s_\nu}^2} \|\frac{\widehat{s_\nu}}{s_\nu} \boldsymbol{\eta}^{j'} - \mathbf{u}^j\|^2\}\,, \\
\boldsymbol{\nabla}_{\mathbf{u}^j}\, p(\mathbf{u}^j) &= \frac{1}{\widehat{s_\nu}^2\, N_d} \sum_{j'=1}^{N_d} (\frac{\widehat{s_\nu}}{s_\nu} \boldsymbol{\eta}^{j'} - \mathbf{u}^j) \\
&\quad \times \exp\{-\frac{1}{2\widehat{s_\nu}^2} \|\frac{\widehat{s_\nu}}{s_\nu} \boldsymbol{\eta}^{j'} - \mathbf{u}^j\|^2\}\,,
\end{aligned}
$$

in which $\widehat{s_\nu}$ is the modified Silverman bandwidth s_ν, which has been introduced in [50],

$$
\widehat{s_\nu} = \frac{s_\nu}{\sqrt{s_\nu^2 + \frac{N_d - 1}{N_d}}} \quad , \quad s_\nu = \left\{ \frac{4}{N_d(2+\nu)} \right\}^{1/(\nu+4)} .
$$

(2) $[\boldsymbol{\mathcal{W}}^{\rm wien}(t)] = [\mathbb{W}^{\rm wien}(t)]\,[a]$ where $\{[\mathbb{W}^{\rm wien}(t)], t \in \mathbb{R}^+\}$ is the $\mathbb{M}_{\nu,N_d}$-valued normalized Wiener process.
(3) $[\boldsymbol{\mathcal{N}}]$ is the $\mathbb{M}_{\nu,N_d}$-valued normalized Gaussian random matrix that is independent of process $[\mathbb{W}^{\rm wien}]$.
(4) The free parameter f_0, such that $0 < f_0 < 4/\widehat{s_\nu}$, allows the dissipation term of the nonlinear second-order dynamic system (dissipative Hamiltonian system) to be controlled in order to kill the transient part induced by the initial conditions. A common value is $f_0 = 4$ (note that $\widehat{s_\nu} < 1$).
(5) We then have $[\mathbf{Z}_{m_{\rm opt}}] = \lim_{t \to +\infty} [\boldsymbol{\mathcal{Z}}(t)]$ in probability distribution. The Störmer-Verlet scheme is used for solving the reduced-order ISDE, which allows for generating the learned

realizations, $[z_{\rm ar}^1], \ldots, [z_{\rm ar}^{n_{\rm MC}}]$, and then, generating the learned realizations $[\eta_{\rm ar}^1], \ldots, [\eta_{\rm ar}^{n_{\rm MC}}]$ such that $[\eta_{\rm ar}^\ell] = [z_{\rm ar}^\ell]\,[g_{m_{\rm opt}}]^T$.
(6) The learned realizations $\{\mathbf{x}_{\rm ar}^{\ell'}, \ell' = 1, \ldots, N_{\rm ar}\}$ of random vector $\mathbf{X}$ are then calculated (see Eq. (A.1)) by $\mathbf{x}_{\rm ar}^{\ell'} = \underline{\mathbf{x}} + [\varphi]\,[\mu]^{1/2}\,\boldsymbol{\eta}_{\rm ar}^{\ell'}$.

(A.6) Constraints on the second-order moments of the components of $\boldsymbol{H}$. In general, the mean value of $\mathbf{H}$ estimated using the $N_{\rm ar}$ learned realizations $\{\boldsymbol{\eta}_{\rm ar}^{\ell'}, \ell' = 1, \ldots, N_{\rm ar}\}$, is sufficiently close to zero. Likewise, the estimate of the covariance matrix of $\mathbf{H}$, which must be the identity matrix, is sufficiently close to a diagonal matrix. However, sometimes the diagonal entries of the estimated covariance matrix can be lower than 1. Normalization can be recovered by imposing constraints

$$\{E\{(H_k)^2\} = 1, k = 1, \ldots, \nu\}\,,$$

in the algorithm presented in paragraph (v). For that, we use the method and the iterative algorithm presented in [72] (that is based on Sections 5.5 and 5.6 of [92]). The constraints are imposed by using the Kullback-Leibler minimum cross-entropy principle. The resulting optimization problem is formulated using a Lagrange multiplier $\mathbf{v} = (v_1, \ldots, v_\nu)$ associated with the constraints. The optimal solution of the Lagrange multiplier is computed using an efficient iterative algorithm. At each iteration, the MCMC generator detailed in paragraph (v) is used. The constraints are rewritten as

$$E\{\mathbf{h}(\mathbf{H})\} = \mathbf{b}\,,$$

in which the function $\mathbf{h} = (h_1, \ldots, h_\nu)$ and the vector $\mathbf{b} = (b_1, \ldots, b_\nu)$ are such that $h_k(\mathbf{H}) = (H_k)^2$ and $b_k = 1$ for k in $\{1, \ldots, \nu\}$. To take into account the constraints in the algorithm of paragraph (v), Eq. (A.6) is replaced by the following one,

$$[L_{\mathbf{v}}([u])]_{kj} = \frac{1}{p(\mathbf{u}^j)}\,\{\boldsymbol{\nabla}_{\mathbf{u}^j}\,p(\mathbf{u}^j)\}_k - 2\,v_k u_k^j\,.$$

The iteration algorithm for computing $\mathbf{v}^{i+1}$ as a function of $\mathbf{v}^i$ is the following,

$$\begin{aligned} \mathbf{v}^{i+1} &= \mathbf{v}^i - \alpha_i[\Gamma''(\mathbf{v}^i)]^{-1}\,\boldsymbol{\Gamma}'(\mathbf{v}^i) \quad , \quad i \geq 0\,, \\ \mathbf{v}^0 &= \mathbf{0}_\nu\,, \end{aligned} \tag{A.7}$$

in which $\boldsymbol{\Gamma}'(\mathbf{v}^i) = \mathbf{b} - E\{\mathbf{h}(\mathbf{H}_{\mathbf{v}^i})\}$ and $[\Gamma''(\mathbf{v}^i)] = [\mathrm{cov}\{\mathbf{h}(\mathbf{H}_{\mathbf{v}^i})\}]$ (the covariance matrix), and where α_i is a relaxation function (less than 1) that is introduced for controlling the convergence as a function of iteration number i. For given $i_2 \geq 2$, for given β_1 and β_2 such that $0 < \beta_1 < \beta_2 \leq 1$, α_i can be defined by:
- for $i \leq i_2$, $\alpha_i = \beta_1 + (\beta_2 - \beta_1)(i-1)/(i_2 - 1)$;
- for $i > i_2$, $\alpha_i = \beta_2$.
The convergence of the iteration algorithm is controlled by the error function $i \mapsto \mathrm{err}(i)$ defined by

$$\mathrm{err}(i) = \|\mathbf{b} - E\{\mathbf{h}(\mathbf{H}_{\mathbf{v}^i})\}\|/\|\mathbf{b}\|\,. \tag{A.8}$$

At each iteration i, $E\{\mathbf{h}(\mathbf{H}_{\mathbf{v}^i})\}$ and $[\mathrm{cov}\{\mathbf{h}(\mathbf{H}_{\mathbf{v}^i})\}]$ are estimated by using the $N_{\rm ar}$ learned realizations of $\mathbf{H}_{m_{\rm opt}}(\mathbf{v}^i)$ obtained by reshaping the learned realizations.

References

[1] O. Ezvan, X. Zeng, R. Ghanem, B. Gencturk, Dominant vibration modes for broadband frequency analysis of multiscale structures with numerous local vibration modes, International Journal for Numerical Methods in Engineering 117 (6) (2019) 644–692. doi:10.1002/nme.5971.

[2] O. Ezvan, X. Zeng, R. Ghanem, B. Gencturk, Multiscale modal analysis of fully-loaded spent nuclear fuel canisters, Computer Methods in Applied Mechanics and Engineering 367 (2020) 113072.

[3] O. Ezvan, X. Zeng, R. Ghanem, B. Gencturk, Dominant substructural vibration modes for fully-loaded spent nuclear fuel canisters, Computational Mechanics 67 (1) (2021) 365–384.

[4] M. A. Grepl, Y. Maday, N. C. Nguyen, A. T. Patera, Efficient reduced-basis treatment of nonaffine and nonlinear partial differential equations, ESAIM: Mathematical Modelling and Numerical Analysis 41 (3) (2007) 575–605. doi:10.1051/m2an:2007031.

[5] N. Nguyen, J. Peraire, An efficient reduced-order modeling approach for non-linear parametrized partial differential equations, International Journal for Numerical Methods in Engineering 76 (1). doi:10.1002/nme.2309.

[6] S. Chaturantabut, D. C. Sorensen, Nonlinear model reduction via discrete empirical interpolation, SIAM Journal on Scientific Computing 32 (5) (2010) 2737–2764.

[7] J. Degroote, J. Virendeels, K. Willcox, Interpolation among reduced-order matrices to obtain parameterized models for design, optimization and probabilistic analysis, nternational Journal for Numerical Methods in Fluids 63 (2010) 207–230. doi:10.1002/fld.2089.

[8] K. Carlberg, C. Bou-Mosleh, C. Farhat, Efficient non-linear model reduction via a least-squares petrov–galerkin projection and compressive tensor approximations, International Journal for Numerical Methods in Engineering 86 (2) (2011) 155–181. doi:10.1002/nme.3050.

[9] K. Carlberg, C. Farhat, A low-cost, goal-oriented compact proper orthogonal decomposition basis for model reduction of static systems, International Journal for Numerical Methods in Engineering 86 (3) (2011) 381–402. doi:10.1002/nme.3074.

[10] D. Amsallem, M. J. Zahr, C. Farhat, Nonlinear model order reduction based on local reduced-order bases, International Journal for Numerical Methods in Engineering 92 (10) (2012) 891–916. doi:10.1002/nme.4371.

[11] K. Carlberg, C. Farhat, J. Cortial, D. Amsallem, The gnat method for nonlinear model reduction: effective implementation and application to computational fluid dynamics and turbulent flows, Journal of Computational Physics 242 (2013) 623–647. doi:10.1016/j.jcp.2013.02.028.

[12] M. Zahr, C. Farhat, Progressive construction of a parametric reduced-order model for pde-constrained optimization, International Journal for Numerical Methods in Engineering 102 (5) (2015) 1077–1110. doi:10.1002/nme.4770.

[13] D. Amsallem, M. Zahr, Y. Choi, C. Farhat, Design optimization using hyper-reduced-order models, Structural and Multidisciplinary Optimization 51 (4) (2015) 919–940. doi:10.1007/s00158-014-1183-y.

[14] K. J. Bathe, E. L. Wilson, Numerical Methods in Finite Element Analysis, Prentice-Hall, New York, 1976.

[15] M. Geradin, D. Rixen, Mechanical Vibrations, Wiley, Chichester, 1997.

[16] R. Ohayon, C. Soize, Advanced Computational Vibroacoustics - Reduced-Order Models and Uncertainty Quantification, Cambridge University Press, New York, 2014.

[17] R. Ohayon, C. Soize, Structural Acoustics and Vibration: Mechanical Models, Variational Formulations and Discretization, Academic Press, San Diego, London, 1998.

[18] O. Ezvan, A. Batou, C. Soize, Multilevel reduced-order computational model in structural dynamics for the low- and medium-frequency ranges, Computers & Structures 160 (2015) 111–125. doi:10.1016/j.compstruc.2015.08.007.

[19] O. Ezvan, A. Batou, C. Soize, L. Gagliardini, Multilevel model reduction for uncertainty quantification in computational structural dynamics, Computational Mechanics 59 (2) (2017) 219–246. doi:10.1007/s00466-016-1348-1.

[20] J. Reyes, C. Desceliers, C. Soize, L. Gagliardini, Multi-frequency model reduction for uncertainty quantification in computational vibroacoutics, Computational Mechanics 69 (2022) 661–682. doi:10.1007/s00466-021-02109-y.

[21] R. Ohayon, C. Soize, Clarification about component mode synthesis methods for substructures with physical flexible interfaces, International Journal of Aeronautical and Space Sciences 15 (2) (2014) 113–122. doi:10.5139/IJASS.2014.15.2.113.

[22] J. H. Argyris, S. Kelsey, The analysis of fuselages of arbitrary cross-section and taper: A dsir sponsored reserach program on the development and application of the matrix force method and the digital computer, Aircraft Engineering and Aerospace Technology 31 (9) (1959) 272–283. doi:10.1108/eb033156.

[23] J. S. Przemieniecki, Matrix structural analysis of substructures, AIAA Journal 1 (1) (1963) 138–147. doi:10.2514/3.1483.

[24] R. J. Guyan, Reduction of stiffness and mass matrices, AIAA Journal (1965) 380–380doi:10.2514/3.2874.

[25] B. Irons, Structural eigenvalue problems - elimination of unwanted variables, AIAA Journal 3 (5) (1965) 961–962. doi:10.2514/3.3027.
[26] W. C. Hurty, Vibrations of structural systems by component mode synthesis, ASCE Journal of Engineering Mechanics 86 (4) (1960) 51–69.
[27] W. C. Hurty, Dynamic analysis of structural systems using component modes, AIAA Journal 3 (4) (1965) 678–685. doi:10.2514/3.2947.
[28] R. Craig, M. Bampton, Coupling of substructures for dynamic analyses, AIAA Journal 6 (7) (1968) 1313–1322. doi:10.2514/3.4741.
[29] A. Bhosekar, M. Ierapetritou, Advances in surrogate based modeling, feasibility analysis, and optimization: A review, Computers & Chemical Engineering 108 (2018) 250–267. doi:10.1016/j.compchemeng.2017.09.017.
[30] B. Nayroles, G. Touzot, P. Villon, Generalizing the finite element method: diffuse approximation and diffuse elements, Computational Mechanics 10 (5) (1992) 307–318. doi:10.1007/BF00364252.
[31] T. Belytschko, Y. Krongauz, D. Organ, M. Fleming, P. Krysl, Meshless methods: an overview and recent developments, Computer Methods in Applied Mechanics and Engineering 139 (1-4) (1996) 3–47. doi:10.1016/S0045-7825(96)01078-X.
[32] C. A. Duarte, J. T. Oden, H-p clouds, an h-p meshless method, Numerical Methods for Partial Differential Equations: An International Journal 12 (6) (1996) 673–705. doi:10.1002/(SICI)1098-2426(199611)12:6<673::AID-NUM3>3.0.CO;2-P.
[33] P. Breitkopf, A. Rassineux, G. Touzot, P. Villon, Explicit form and efficient computation of MLS shape functions and their derivatives, International Journal for Numerical Methods in Engineering 48 (3) (2000) 451–466. doi:10.1002/(SICI)1097-0207(20000530)48:3<451::AID-NME892>3.0.CO;2-1.
[34] A. Rassineux, P. Villon, J.-M. Savignat, O. Stab, Surface remeshing by local Hermite diffuse interpolation, International Journal for numerical methods in Engineering 49 (1-2) (2000) 31–49. doi:10.1002/1097-0207(20000910/20)49:1/23.0.CO;2-6.
[35] X. Zhang, K. Z. Song, M. W. Lu, X. Liu, Meshless methods based on collocation with radial basis functions, Computational mechanics 26 (4) (2000) 333–343. doi:10.1007/s004660000181.
[36] R. Ghanem, D. Higdon, H. Owhadi, Handbook of Uncertainty Quantification, Vol. 1 to 3, Springer, Cham, Switzerland, 2017. doi:10.1007/978-3-319-12385-1.
[37] C. Soize, Uncertainty Quantification. An Accelerated Course with Advanced Applications in Computational Engineering, Springer, New York, 2017. doi:10.1007/978-3-319-54339-0.
[38] J. P. Kleijnen, Kriging metamodeling in simulation: A review, European Journal of Operational Research 192 (3) (2009) 707–716. doi:10.1016/j.ejor.2007.10.013.
[39] V. Dubourg, B. Sudret, J.-M. Bourinet, Reliability-based design optimization using kriging surrogates and subset simulation, Structural and Multidisciplinary Optimization 44 (5) (2011) 673–690. doi:10.1007/s00158-011-0653-8.
[40] P. Kersaudy, B. Sudret, N. Varsier, O. Picon, J. Wiart, A new surrogate modeling technique combining kriging and polynomial chaos expansions–application to uncertainty analysis in computational dosimetry, Journal of Computational Physics 286 (2015) 103–117.
[41] R. Ghanem, P. D. Spanos, Stochastic Finite Elements: a Spectral Approach, Springer-Verlag, New York, 1991.
[42] D. Xiu, G. E. Karniadakis, The Wiener-Askey polynomial chaos for stochastic differential equations, SIAM Journal on Scientific Computing 24 (2) (2002) 619–644. doi:10.1137/S1064827501387826.
[43] C. Soize, R. Ghanem, Physical systems with random uncertainties: chaos representations with arbitrary probability measure, SIAM Journal on Scientific Computing 26 (2) (2004) 395–410. doi:10.1137/S1064827503424505.
[44] X. Wan, G. E. Karniadakis, Multi-element generalized polynomial chaos for arbitrary probability measures, SIAM Journal on Scientific Computing 28 (3) (2006) 901–928. doi:10.1137/050627630.
[45] C. Soize, C. Desceliers, Computational aspects for constructing realizations of polynomial chaos in high dimension, SIAM Journal on Scientific Computing 32 (5) (2010) 2820–2831. doi:10.1137/100787830.
[46] G. Blatman, B. Sudret, Adaptive sparse polynomial chaos expansion based on least angle regression, Journal of Computational Physics 230 (6) (2011) 2345–2367. doi:10.1016/j.jcp.2010.12.021.
[47] G. Perrin, C. Soize, D. Duhamel, C. Funfschilling, Identification of polynomial chaos representations in high dimension from a set of realizations, SIAM Journal on Scientific Computing 34 (6) (2012) A2917–A2945. doi:10.1137/11084950X.
[48] R. Tipireddy, R. Ghanem, Basis adaptation in homogeneous chaos spaces, Journal of Computational Physics 259 (2014) 304–317. doi:10.1016/j.jcp.2013.12.009.
[49] M. Babaei, A. Alkhatib, I. Pan, Robust optimization of subsurface flow using polynomial chaos and response surface surrogates, Computational Geosciences 19 (2015) 979–998.
[50] C. Soize, Polynomial chaos expansion of a multimodal random vector, SIAM-ASA Journal on Uncertainty Quan-

tification 3 (1) (2015) 34–60. doi:10.1137/140968495.
[51] S. Abraham, M. Raisee, G. Ghorbanias, F. Contino, C. Lacor, A robust and efficient stepwise regression method for building sparse polynomial chaos expansions, Journal of Computational Physics 332 (2017) 461–474. doi:10.1016/j.jcp.2016.12.015.
[52] N. Luthen, S. Marelli, B. Sudret, Sparse polynomial chaos expansions: Literature survey and benchmark, SIAM/ASA Journal on Uncertainty Quantification 9 (2) (2021) 593–649. doi:10.1137/20M1315774.
[53] C. Soize, R. Ghanem, Polynomial chaos representation of databases on manifolds, Journal of Computational Physics 335 (2017) 201–221. doi:10.1016/j.jcp.2017.01.031.
[54] J. M. Bernardo, A. F. M. Smith, Bayesian Theory, John Wiley & Sons, Chichester, 2000.
[55] M. C. Kennedy, A. O'Hagan, Bayesian calibration of computer models, Journal of the Royal Statistical Society: Series B (Statistical Methodology) 63 (3) (2001) 425–464. doi:10.1111/1467-9868.00294.
[56] P. Congdon, Bayesian Statistical Modelling, Vol. 704, John Wiley & Sons, 2007.
[57] B. P. Carlin, T. A. Louis, Bayesian Methods for Data Analysis, Chapman and Hall/CRC, 2008.
[58] J. Marin, P. Pudlo, C. Robert, R. Ryder, Approximate Bayesian computational methods, Statistics and Computing 22 (6) (2012) 1167–1180. doi:10.1007/s11222-011-9288-2.
[59] S. L. Scott, A. W. Blocker, F. V. Bonassi, H. A. Chipman, E. I. George, R. E. McCulloch, Bayes and big data: The consensus monte carlo algorithm, International Journal of Management Science and Engineering Management 11 (2) (2016) 78–88. doi:10.1080/17509653.2016.1142191.
[60] C. Soize, R. Ghanem, C. Desceliers, Sampling of Bayesian posteriors with a non-Gaussian probabilistic learning on manifolds from a small dataset, Statistics and Computing 30 (5) (2020) 1433–1457. doi:10.1007/s11222-020-09954-6.
[61] Y. M. Marzouk, H. N. Najm, L. A. Rahn, Stochastic spectral methods for efficient Bayesian solution of inverse problems, Journal of Computational Physics 224 (2) (2007) 560–586. doi:10.1016/j.jcp.2006.10.010.
[62] A. M. Stuart, Inverse problems: a Bayesian perspective, Acta Numerica 19 (2010) 451–559. doi:10.1017/S0962492910000061.
[63] C. Soize, A computational inverse method for identification of non-Gaussian random fields using the Bayesian approach in very high dimension, Computer Methods in Applied Mechanics and Engineering 200 (45-46) (2011) 3083–3099. doi:10.1016/j.cma.2011.07.005.
[64] M. Dashti, A. M. Stuart, The Bayesian approach to inverse problems, in: R. Ghanem, D. Higdon, O. Houman (Eds.), Handbook of Uncertainty Quantification, Springer, Cham, Switzerland, 2017, Ch. 10, pp. 311–428. doi:10.1007/978-3-319-12385-1_7.
[65] M. Arnst, B. Abello Álvarez, J.-P. Ponthot, R. Boman, Itô-SDE MCMC method for Bayesian characterization of errors associated with data limitations in stochastic expansion methods for uncertainty quantification, Journal of Computational Physics 349 (2017) 59–79. doi:10.1016/j.jcp.2017.08.005.
[66] G. Perrin, C. Soize, Adaptive method for indirect identification of the statistical properties of random fields in a Bayesian framework, Computational Statistics 35 (1) (2020) 111–133. doi:10.1007/s00180-019-00936-5.
[67] S. Russel, P. Norvig, Artifical Intelligence, A Modern Approach, Third Edition, Pearson, Harlow, 2016.
[68] K. Gurney, An introduction to Neural Networks, CRC Press, LOndon, 1997. doi:10.1201/9781315273570.
[69] Y. LeCun, Y. Bengio, G. Hinton, Deep learning, Nature 521 (2015) 436–444. doi:10.1038/nature14539.
[70] C. Soize, R. Ghanem, Data-driven probability concentration and sampling on manifold, Journal of Computational Physics 321 (2016) 242–258. doi:10.1016/j.jcp.2016.05.044.
[71] C. Soize, R. Ghanem, Probabilistic learning on manifolds, Foundations of Data Science 2 (3) (2020) 279–307. doi:10.3934/fods.2020013.
[72] C. Soize, R. Ghanem, Probabilistic learning on manifolds (plom) with partition, International Journal for Numerical Methods in Engineering 123 (1) (2022) 268–290. doi:10.1002/nme.6856.
[73] A. Talwalkar, S. Kumar, H. Rowley, Large-scale manifold learning, in: 2008 IEEE Conference on Computer Vision and Pattern Recognition, IEEE, 2008, pp. 1–8. doi:10.1109/CVPR.2008.4587670.
[74] D. Gorissen, I. Couckuyt, P. Demeester, T. Dhaene, K. Crombecq, A surrogate modeling and adaptive sampling toolbox for computer based design, Journal of Machine Learning Research 11 (68) (2010) 2051–2055.
[75] A. C. Öztireli, M. Alexa, M. Gross, Spectral sampling of manifolds, ACM Transactions on Graphics (TOG) 29 (6) (2010) 1–8. doi:10.1145/1882261.1866190.
[76] Y. Marzouk, T. Moselhy, M. Parno, A. Spantini, Sampling via measure transport: An introduction, Handbook of uncertainty quantification (2016) 1–41doi:10.1007/978-3-319-11259-6_23-1.
[77] M. D. Parno, Y. M. Marzouk, Transport map accelerated markov chain Monte Carlo, SIAM/ASA Journal on Uncertainty Quantification 6 (2) (2018) 645–682. doi:10.1137/17M1134640.
[78] G. Perrin, C. Soize, N. Ouhbi, Data-driven kernel representations for sampling with an unknown block dependence structure under correlation constraints, Computational Statistics & Data Analysis 119 (2018) 139–154. doi:10.1016/j.csda.2017.10.005.
[79] P. Tsilifis, R. Ghanem, Bayesian adaptation of chaos representations using variational inference and sampling on

geodesics, Proceedings of the Royal Society A: Mathematical, Physical and Engineering Sciences 474 (2217) (2018) 20180285. doi:10.1098/rspa.2018.0285.

[80] Y. Kevrekidis, Manifold learning for parameter reduction, Bulletin of the American Physical Society 65. doi:10.1016/j.jcp.2019.04.015.

[81] R. Ghanem, C. Soize, Probabilistic nonconvex constrained optimization with fixed number of function evaluations, International Journal for Numerical Methods in Engineering 113 (4) (2018) 719–741. doi:10.1002/nme.5632.

[82] R. Ghanem, C. Soize, C. Thimmisetty, Optimal well-placement using probabilistic learning, Data-Enabled Discovery and Applications 2 (1) (2018) 1–16. doi:10.1007/s41688-017-0014-x.

[83] C. Soize, Design optimization under uncertainties of a mesoscale implant in biological tissues using a probabilistic learning algorithm, Computational Mechanics 62 (3) (2018) 477–497. doi:10.1007/s00466-017-1509-x.

[84] R. Ghanem, C. Soize, C. Safta, X. Huan, G. Lacaze, J. C. Oefelein, H. N. Najm, Design optimization of a scramjet under uncertainty using probabilistic learning on manifolds, Journal of Computational Physics 399 (2019) 108930. doi:10.1016/j.jcp.2019.108930.

[85] J. O. Almeida, F. A. Rochinha, A probabilistic learning approach applied to the optimization of wake steering in wind farms, Journal of Computing and Information Science in Engineering 23 (1) (2022) 011003. doi:10.1115/1.4054501.

[86] R. Ghanem, C. Soize, L. Mehrez, V. Aitharaju, Probabilistic learning and updating of a digital twin for composite material systems, International Journal for Numerical Methods in Engineeringdoi:10.1002/nme.6430.

[87] M. Arnst, C. Soize, K. Bulthies, Computation of sobol indices in global sensitivity analysis from small data sets by probabilistic learning on manifolds, International Journal for Uncertainty Quantification 11 (2) (2021) 1–23. doi:10.1615/Int.J.UncertaintyQuantification.2020032674.

[88] C. Farhat, R. Tezaur, T. Chapman, P. Avery, C. Soize, Feasible probabilistic learning method for model-form uncertainty quantification in vibration analysis, AIAA Journal 57 (11) (2019) 4978–4991. doi:10.2514/1.J057797.

[89] C. Soize, R. Ghanem, C. Safta, X. Huan, Z. P. Vane, J. C. Oefelein, G. Lacaze, H. N. Najm, Enhancing model predictability for a scramjet using probabilistic learning on manifolds, AIAA Journal 57 (1) (2019) 365–378. doi:10.2514/1.J057069.

[90] C. Soize, C. Farhat, Probabilistic learning for modeling and quantifying model-form uncertainties in nonlinear computational mechanics, International Journal for Numerical Methods in Engineering 117 (2019) 819–843. doi:10.1002/nme.5980.

[91] J. Guilleminot, J. E. Dolbow, Data-driven enhancement of fracture paths in random composites, Mechanics Research Communications 103 (2020) 103443. doi:10.1016/j.mechrescom.2019.103443.

[92] C. Soize, R. Ghanem, Physics-constrained non-Gaussian probabilistic learning on manifolds, International Journal for Numerical Methods in Engineering 121 (1) (2020) 110–145. doi:10.1002/nme.6202.

[93] C. Soize, R. Ghanem, Probabilistic learning on manifolds constrained by nonlinear partial differential equations for small datasets, Computer Methods in Applied Mechanics and Engineering 380 (2021) 113777. doi:10.1016/j.cma.2021.113777.

[94] T. Duong, M. L. Hazelton, Cross-validation bandwidth matrices for multivariate kernel density estimation, Scandinavian Journal of Statistics 32 (3) (2005) 485–506. doi:10.1111/j.1467-9469.2005.00445.x.

[95] T. Duong, A. Cowling, I. Koch, M. Wand, Feature significance for multivariate kernel density estimation, Computational Statistics & Data Analysis 52 (9) (2008) 4225–4242. doi:10.1016/j.csda.2008.02.035.

[96] M. Filippone, G. Sanguinetti, Approximate inference of the bandwidth in multivariate kernel density estimation, Computational Statistics & Data Analysis 55 (12) (2011) 3104–3122. doi:10.1016/j.csda.2011.05.023.

[97] N. Zougab, S. Adjabi, C. C. Kokonendji, Bayesian estimation of adaptive bandwidth matrices in multivariate kernel density estimation, Computational Statistics & Data Analysis 75 (2014) 28–38. doi:10.1016/j.csda.2014.02.002.

[98] I. Zelinka, V. Snasael, A. Abraham, Handbook of optimization: from classical to modern approach, Vol. 38, Springer Science & Business Media, 2013.

[99] Y. LeCun, L. Bottou, Y. Bengio, P. Haffner, Gradient-based learning applied to document recognition, Proceedings of the IEEE 86 (11) (1998) 2278–2324. doi:10.1109/5.726791.

[100] J. C. Spall, Introduction to Stochastic Search and Optimization: Estimation, Simulation, and Control, Vol. 65, John Wiley & Sons, 2005.

[101] C. C. Coello, Evolutionary multi-objective optimization: a historical view of the field, IEEE Computational Intelligence Magazine 1 (1) (2006) 28–36. doi:10.1109/MCI.2006.1597059.

[102] A. Konak, D. W. Coit, A. E. Smith, Multi-objective optimization using genetic algorithms: A tutorial, Reliability Engineering & System Safety 91 (9) (2006) 992–1007. doi:10.1016/j.ress.2005.11.018.

[103] C. Soize, A. Batou, Stochastic reduced-order model in low-frequency dynamics in presence of numerous local elastic modes, Journal of applied mechanics 78 (6). doi:10.1115/1.4002593.

[104] J. Guilleminot, C. Soize, On the statistical dependence for the components of random elasticity tensors exhibiting material symmetry properties, Journal of Elasticity 111 (2) (2013) 109–130. doi:10.1007/s10659-012-9396-z.

[105] R. Coifman, S. Lafon, Diffusion maps, Applied and Computational Harmonic Analysis 21 (1) (2006) 5–30. doi:10.1016/j.acha.2006.04.006.

[106] S. Lafon, A. B. Lee, Diffusion maps and coarse-graining: A unified framework for dimensionality reduction, graph partitioning, and data set parameterization, IEEE transactions on pattern analysis and machine intelligence 28 (9) (2006) 1393–1403. doi:10.1109/TPAMI.2006.184.